

EW D-optimal Designs for Experiments with Mixed Factors

Siting Lin¹, Yifei Huang², and Jie Yang¹

¹University of Illinois at Chicago and ²Astellas Pharma, Inc.

May 2, 2025

Abstract

We consider EW D-optimal designs as robust designs for experiments under a general parametric model with discrete and continuous factors. When a pilot study is available, we recommend sample-based EW D-optimal designs for subsequent experiments. Otherwise, we recommend EW D-optimal designs under a prior distribution for model parameters. We propose an EW ForLion algorithm for finding EW D-optimal designs under a general parametric model, and justify that the designs found by our algorithm are EW D-optimal. To facilitate potential users in practice, we also develop a rounding algorithm that converts an approximate design with mixed factors to an exact design with prespecified grid points and the number of experimental units. By applying our algorithms for real experiments under multinomial logistic models or generalized linear models, we show that our designs are highly efficient with respect to locally D-optimal designs and more robust against parameter value misspecifications.

Key words and phrases: EW ForLion algorithm, Exact design, Mixed factors, Generalized linear model, Multinomial logistic model, Robust experimental design

1. Introduction

In this paper, we consider robust designs for experiments with discrete and continuous factors. A motivating example is the paper feeder experiment described in Joseph and Wu (2004). The goal was to ensure precise feeding of one sheet of paper each time to a copier. Two common failure modes are frequently observed, namely *misfeed* when the feeder fails to feed any sheet of paper, and *multifeed* when the feeder picks up more than one sheets of paper at a time. The experiment involves eight discrete control factors (see Table 2 in Joseph and Wu (2004)) and one continuous variable, the stack force. The responses fall into three mutually exclusive categories, namely **misfeed** (typically with low stack force), **normal**, and **multifeed** (typically with high stack force). The results of a previous experiment were listed in Table 3 of Joseph and Wu (2004). The original design was conducted via a control array modified from $OA(18, 2^1 \times 3^7)$ (see Table 5 in Joseph and Wu (2004)) for the eight discrete factors and an essentially uniform allocation on a

predetermined set of discrete levels of the continuous factor. If a subsequent experiment will be conducted to study the factor effects, how can we do better?

In the original analysis by Joseph and Wu (2004), two generalized linear models with probit link (McCullagh and Nelder, 1989; Dobson and Barnett, 2018) were used to model `misfeed` and `multifeed` separately. However, since `misfeed` and `multifeed` do not occur simultaneously and are both possible outcomes of the experiment, it would be more appropriate to adopt one multinomial model rather than two separate binomial models, so that the factor effects can be estimated more precisely due to the combined data and also be comparable for different types of failures. In this study, we adopt the multinomial logistic models (Glonek and McCullagh, 1995; Zocchi and Atkinson, 1999; Bu et al., 2020) for analyzing the paper feeder experiment, which include baseline-category (or known as multiclass logistic), cumulative, adjacent-categories, and continuation-ratio logit models.

For experiments with discrete factors only, many numerical algorithms have been proposed for finding optimal designs, including Fedorov-Wynn (Fedorov, 1972; Fedorov and Hackl, 1997), multiplicative (Titterton, 1976, 1978; Silvey et al., 1978), cocktail (Yu, 2010), lift-one (Yang and Mandal, 2015; Yang et al., 2017; Bu et al., 2020), as well as classical optimization techniques (see Huang et al. (2024) for a review). For experiments with continuous factors only, Ai et al. (2023) incorporated the Fedorov-Wynn algorithm with the lift-one algorithm for continuation-ratio link models, Yang et al. (2013) and Harman et al. (2020) discretized the continuous factors into grid points and treated the experiments as with discrete factors.

For experiments with mixed factors, particle swarm optimization (PSO) algorithms have been applied for D-optimal designs under generalized linear models with binary responses (Lukemire et al., 2019) and cumulative logit models (Lukemire et al., 2022), which, however, cannot guarantee the optimal solution to be ever found (Kennedy and Eberhart, 1995; Poli et al., 2007). Huang et al. (2024) proposed a ForLion algorithm, which added a merging step to Ai et al. (2023)’s algorithm and significantly reduced the number of design points. Unlike PSO-types of algorithms, the ForLion algorithm is guaranteed to find D-optimal designs based on the general equivalence theorem (Kiefer, 1974; Pukelsheim, 1993; Atkinson et al., 2007; Stufken and Yang, 2012; Fedorov and Leonov, 2014).

The ForLion algorithm has been successfully applied to both generalized linear models and multinomial logistic models with mixed factors (Huang et al., 2024). However, it relies on pre-assumed parameter values and produces designs known as *locally optimal* (Chernoff, 1953), which may not be robust when the experimenters are uncertain about the parameter values. To address the limitation due to local optimality, Bayesian D-optimal designs have been proposed (Chaloner and Verdinelli, 1995), which maximize $E(\log |\mathbf{F}|)$ with respect to a prior distribution on unknown parameters, where \mathbf{F} is the Fisher information matrix associated with the design. However, a major drawback of Bayesian D-optimal designs is its computational intensity, even with D-criterion that maximizes the determinant of the Fisher information matrix. As a promising alternative, Expected Weighted (EW) D-optimal designs have been proposed for generalized linear models (Yang et al., 2016), cumulative link models (Yang et al., 2017), and multinomial logistic models (Bu et al., 2020) with discrete factors, which maximize $\log |E(\mathbf{F})|$

or equivalently $|E(\mathbf{F})|$. Compared with Bayesian D-optimal designs, EW D-optimal designs are computationally much faster and often highly efficient in terms of the Bayesian criterion (Yang et al., 2016, 2017; Bu et al., 2020). Along this line, Tong et al. (2014) provided analytical solutions for certain cases of EW D-optimal designs for generalized linear models, and Bu et al. (2020) incorporated the lift-one and exchange algorithms with the EW criterion.

In this paper, we adopt EW D-criterion and adapt the ForLion algorithm for finding robust designs with mixed factors. The original EW D-optimal designs were proposed for experiments with discrete factors or discretized continuous factors. To solve our problems, we formulate in Section 2 the EW D-optimal criterion and characterize EW D-optimal designs for general parametric statistical models with mixed factors. In Section 3, we develop algorithms for finding two types of EW D-optimal designs with mixed factors, namely sample-based EW D-optimal designs for experiments with a pilot study, and integral-based EW D-optimal designs for experiments with a prior distribution of unknown parameters. We further formulate EW D-optimal designs for multinomial logistic models and generalized linear models, and propose an algorithm for converting approximate designs with mixed factors to exact designs with grid points. In Section 4, we construct the proposed robust designs for two real experiments, namely the paper feeder experiment (Joseph and Wu, 2004), and an experiment on minimizing surface defects (Wu, 2008). In Section 5, we conclude our findings. The algorithms are implemented in R with version 4.4.2 and the simulations are run on a Windows 11 laptop with 32GB of RAM and a 13th Gen Intel Core i7-13700HX processor.

2. EW D-optimal Designs with Mixed Factors

Following Huang et al. (2024), we consider experiments with a design region $\mathcal{X} = \prod_{j=1}^d I_j \subset \mathbb{R}^d$, where I_j is either a closed finite interval for the first k factors, or a finite set of distinct numerical levels for $k+1 \leq j \leq d$. In both cases, we denote $a_j = \min I_j > -\infty$ and $b_j = \max I_j < \infty$. Note that \mathcal{X} here is compact, which is common for typical applications. If $k=0$, all factors are discrete or qualitative; if $k=d$, all factors are continuous.

Given an experimental setting $\mathbf{x}_i = (x_{i1}, \dots, x_{id})^T \in \mathcal{X}$, suppose there are $n_i \geq 0$ experimental units assigned to this experimental setting. Their responses (could be vectors) are assumed to be iid from a parametric model $M(\mathbf{x}_i, \boldsymbol{\theta})$, where the parameter vector $\boldsymbol{\theta} \in \boldsymbol{\Theta} \subseteq \mathbb{R}^p$ with the parameter space $\boldsymbol{\Theta}$. Suppose the responses are independent across different experimental settings. Under regularity conditions (see, e.g., Sections 2.5 and 2.6 in Lehmann and Casella (1998)), the corresponding Fisher information matrix can be written as $\sum_{i=1}^m n_i \mathbf{F}(\mathbf{x}_i, \boldsymbol{\theta})$, with respect to the corresponding design $\{(\mathbf{x}_i, n_i), i = 1, \dots, m\}$, known as an *exact design*, where $\mathbf{F}(\mathbf{x}_i, \boldsymbol{\theta})$ is a $p \times p$ matrix, known as the Fisher information at \mathbf{x}_i . In design theory, $\boldsymbol{\xi} = \{(\mathbf{x}_i, w_i), i = 1, \dots, m\}$ with $w_i = n_i/n \geq 0$ and $n = \sum_{i=1}^m n_i$, known as an *approximate design*, is often considered first (Kiefer, 1974; Pukelsheim, 1993; Atkinson et al., 2007), which is easier to find. The collection of all feasible designs is denoted by $\Xi = \{(\mathbf{x}_i, w_i), i = 1, \dots, m \mid m \geq 1, \mathbf{x}_i \in \mathcal{X}, w_i \geq 0, \sum_{i=1}^m w_i = 1\}$.

2.1 EW D-optimal designs

Following Bu et al. (2020) and Huang et al. (2024), we adopt the D-criterion for optimal designs. When $\boldsymbol{\theta}$ is given or assumed to be known, the $\boldsymbol{\xi} \in \Xi$ that maximizes $f(\boldsymbol{\xi}) = |\mathbf{F}(\boldsymbol{\xi}, \boldsymbol{\theta})|$ is known as a *locally D-optimal* approximate design (Chernoff, 1953), where $\mathbf{F}(\boldsymbol{\xi}, \boldsymbol{\theta}) = \sum_{i=1}^m w_i \mathbf{F}(\mathbf{x}_i, \boldsymbol{\theta})$ is the Fisher information matrix associated with the design $\boldsymbol{\xi}$. The ForLion algorithm was proposed for finding locally D-optimal approximate designs with mixed factors (Huang et al., 2024).

When $\boldsymbol{\theta}$ is unknown while a prior distribution or probability measure $Q(\cdot)$ on Θ is available instead, we adopt the EW D-optimality (Atkinson et al., 2007; Yang et al., 2016, 2017; Bu et al., 2020; Huang et al., 2025) and look for $\boldsymbol{\xi} \in \Xi$ maximizing

$$f_{\text{EW}}(\boldsymbol{\xi}) = |E\{\mathbf{F}(\boldsymbol{\xi}, \Theta)\}| = \left| \sum_{i=1}^m w_i E\{\mathbf{F}(\mathbf{x}_i, \Theta)\} \right|, \quad (1)$$

called an *integral-based EW D-optimal* approximate design, where

$$E\{\mathbf{F}(\mathbf{x}_i, \Theta)\} = \int_{\Theta} \mathbf{F}(\mathbf{x}_i, \boldsymbol{\theta}) Q(d\boldsymbol{\theta}) \quad (2)$$

is a $p \times p$ matrix after entry-wise expectation with respect to $Q(\cdot)$ on Θ . By replacing $\boldsymbol{\theta}$ in $\mathbf{F}(\boldsymbol{\xi}, \boldsymbol{\theta})$ with Θ , we indicate that the expectation $E\{\mathbf{F}(\boldsymbol{\xi}, \Theta)\}$ is taken with respect to a random parameter vector.

When $\boldsymbol{\theta}$ is unknown but a dataset from a prior or pilot study is available, following Bu et al. (2020) and Huang et al. (2025), we bootstrap the original dataset to obtain a set of bootstrapped datasets, and the corresponding estimated parameter vectors $\{\hat{\boldsymbol{\theta}}_1, \dots, \hat{\boldsymbol{\theta}}_B\}$ by fitting the parametric model on each of the bootstrapped datasets. In other words, we may replace the prior distribution $Q(\cdot)$ in (2) with the empirical distribution of $\{\hat{\boldsymbol{\theta}}_1, \dots, \hat{\boldsymbol{\theta}}_B\}$. That is, we may look for $\boldsymbol{\xi} \in \Xi$ maximizing

$$f_{\text{SEW}}(\boldsymbol{\xi}) = |\hat{E}\{\mathbf{F}(\boldsymbol{\xi}, \Theta)\}| = \left| \sum_{i=1}^m w_i \hat{E}\{\mathbf{F}(\mathbf{x}_i, \Theta)\} \right|, \quad (3)$$

called a *sample-based EW D-optimal* approximate design, where

$$\hat{E}\{\mathbf{F}(\mathbf{x}_i, \Theta)\} = \frac{1}{B} \sum_{j=1}^B \mathbf{F}(\mathbf{x}_i, \hat{\boldsymbol{\theta}}_j) \quad (4)$$

is a bootstrapped estimate of $E\{\mathbf{F}(\mathbf{x}_i, \Theta)\}$ based on $\{\hat{\boldsymbol{\theta}}_1, \dots, \hat{\boldsymbol{\theta}}_B\}$. According to Bu et al. (2020), the EW D-optimal design obtained via bootstrapped samples is a good approximation to the Bayesian D-optimal design obtained in a similar way.

For multinomial logistic models, such as the cumulative logit model used for the trauma clinical trial (see Example 5.2 in Bu et al. (2020)), the feasible parameter space $\Theta = \{\boldsymbol{\theta} = (\beta_{11}, \beta_{12}, \beta_{21}, \beta_{22}, \beta_{31}, \beta_{32}, \beta_{41}, \beta_{42})^T \mid \beta_{11} + \beta_{12}x < \beta_{21} + \beta_{22}x < \beta_{31} + \beta_{32}x < \beta_{41} + \beta_{42}x, \text{ for all } x \in \mathcal{X}\}$ is not rectangular, which makes the integral in (2) difficult to handle. In this case, even with a prior distribution instead of a dataset, we may also draw

a random sample $\{\hat{\boldsymbol{\theta}}_1, \dots, \hat{\boldsymbol{\theta}}_B\}$ from the prior distribution, and adopt the sample-based EW D-optimality. According to Section S6 in the Supplementary Material, in terms of relative efficiency, the obtained EW D-optimal designs are fairly stable against the random samples.

2.2 Characteristics of EW D-optimal designs

In this section, to characterize EW D-optimal designs, we fix either a prior distribution $Q(\cdot)$ on $\boldsymbol{\Theta}$ for integral-based EW D-optimality or a set of bootstrapped or sampled parameter vectors $\{\hat{\boldsymbol{\theta}}_1, \dots, \hat{\boldsymbol{\theta}}_B\}$ for sample-based EW D-optimality, so that either $E\{\mathbf{F}(\mathbf{x}_i, \boldsymbol{\Theta})\}$ is defined as in (2), or $\hat{E}\{\mathbf{F}(\mathbf{x}_i, \boldsymbol{\Theta})\}$ is defined as in (4).

For sample-based EW D-optimal designs under general parametric models, we need the regularity conditions (A1), (A2), and (B3) described in Section 2.4 of Fedorov and Leonov (2014). For integral-based EW D-optimal designs defined as in (1), we need an additional assumption (A3) (see Section S2 in the Supplementary Material).

Theorem 2.1. *For sample-based EW D-optimality under Assumptions (A1), (A2), and (B3), or integral-based EW D-optimality under Assumptions (A1), (A3), and (B3),*

- (i) *there exists an optimal design $\boldsymbol{\xi}^*$ that contains no more than $p(p+1)/2$ design points;*
- (ii) *the set of optimal designs is convex;*
- (iii) *a design $\boldsymbol{\xi}$ is EW D-optimal if and only if $\max_{\mathbf{x} \in \mathcal{X}} d(\mathbf{x}, \boldsymbol{\xi}) \leq p$, where*

$$d(\mathbf{x}, \boldsymbol{\xi}) = \begin{cases} \text{tr}([E\{\mathbf{F}(\boldsymbol{\xi}, \boldsymbol{\Theta})\}]^{-1}E\{\mathbf{F}(\mathbf{x}, \boldsymbol{\Theta})\}), & \text{for integral-based EW D-optimality;} \\ \text{tr}([\hat{E}\{\mathbf{F}(\boldsymbol{\xi}, \boldsymbol{\Theta})\}]^{-1}\hat{E}\{\mathbf{F}(\mathbf{x}, \boldsymbol{\Theta})\}), & \text{for sample-based EW D-optimality.} \end{cases}$$

The proof of Theorem 2.1, as well as proofs of other theorems in this paper, is relegated to Section S4 in the Supplementary Material.

3. Algorithms for EW D-optimal Designs

3.1 Lift-one algorithm for EW D-optimal designs with discrete factors only

When all factors are discrete, that is, each I_j is a finite set of numerical levels and the design region $\mathcal{X} = \prod_{j=1}^d I_j$ contains only a finite number of distinct experimental settings. In this case, we may denote $m = \prod_{j=1}^d |I_j|$ and the corresponding design settings as $\mathbf{x}_1, \dots, \mathbf{x}_m$. The EW D-optimal design problem in this case is to find $\mathbf{w}^* = (w_1^*, \dots, w_m^*)^T \in S = \{(w_1, \dots, w_m)^T \in \mathbb{R}^m \mid w_i \geq 0, i = 1, \dots, m; \sum_{i=1}^m w_i = 1\}$, which maximizes $f_{\text{EW}}(\mathbf{w}) = |\sum_{i=1}^m w_i E\{\mathbf{F}(\mathbf{x}_i, \boldsymbol{\Theta})\}|$ or $f_{\text{SEW}}(\mathbf{w}) = |\sum_{i=1}^m w_i \hat{E}\{\mathbf{F}(\mathbf{x}_i, \boldsymbol{\Theta})\}|$.

The original lift-one algorithm under a general setup (see Algorithm 3 in the Supplementary Material of Huang et al. (2025)) can be used for finding EW D-optimal designs, with $f(\mathbf{w})$ replaced by $f_{\text{EW}}(\mathbf{w})$ or $f_{\text{SEW}}(\mathbf{w})$, called *EW lift-one algorithm*.

To speed up the lift-one algorithm, Yang and Mandal (2015) provided analytic solutions in their Lemma 4.2 for generalized linear models. Bu et al. (2020) mentioned but with no detail that the corresponding optimization problems for multinomial logistic models (MLM) also have analytic solutions when the number of response categories $J \leq 5$. In Section S1 of the Supplementary Material, we provide all the relevant formulae for the lift-one algorithm under an MLM with $J \leq 5$.

3.2 EW ForLion algorithm for EW D-optimal designs with mixed factors and a rounding algorithm for obtaining exact designs

When at least one factor is continuous, that is, at least $I_1 = [a_1, b_1]$, we follow the ForLion algorithm proposed by Huang et al. (2024) for locally D-optimal designs, to find EW D-optimal designs, called the *EW ForLion algorithm* (see Algorithm 1).

When there is no confusion, we may denote (i) $\mathbf{F}(\boldsymbol{\xi})$ for $E\{\mathbf{F}(\boldsymbol{\xi}, \boldsymbol{\Theta})\}$ under integral-based EW D-optimality or $\hat{E}\{\mathbf{F}(\boldsymbol{\xi}, \boldsymbol{\Theta})\}$ under sample-based EW D-optimality, for each $\boldsymbol{\xi} \in \Xi$; and (ii) $\mathbf{F}_{\mathbf{x}}$ for $E\{\mathbf{F}(\mathbf{x}, \boldsymbol{\Theta})\}$ under integral-based EW D-optimality or $\hat{E}\{\mathbf{F}(\mathbf{x}, \boldsymbol{\Theta})\}$ under sample-based EW D-optimality, for each $\mathbf{x} \in \mathcal{X}$. As a result, $d(\mathbf{x}, \boldsymbol{\xi})$ in Theorem 2.1 can be simplified to $d(\mathbf{x}, \boldsymbol{\xi}) = \text{tr}(\mathbf{F}(\boldsymbol{\xi})^{-1}\mathbf{F}_{\mathbf{x}})$ (see Section S3 in the Supplementary Material on relevant efficient calculations).

Algorithm 1: EW ForLion Algorithm

Step 1: Specify the merging threshold $\delta > 0$ (e.g., 10^{-2}) and the converging threshold $\epsilon > 0$ (e.g., 10^{-6}), and establish an initial design $\boldsymbol{\xi}_0 = \{(\mathbf{x}_i^{(0)}, w_i^{(0)}), i = 1, \dots, m_0\} \in \Xi$, such that, $\|\mathbf{x}_i^{(0)} - \mathbf{x}_j^{(0)}\| \geq \delta$ for all $i \neq j$, and $|\mathbf{F}(\boldsymbol{\xi}_0)| > 0$.

Step 2: Merging close design points: Given $\boldsymbol{\xi}_t = \{(\mathbf{x}_i^{(t)}, w_i^{(t)}), i = 1, \dots, m_t\} \in \Xi$ obtained at the t th iteration, detect if there are any two points $\mathbf{x}_i^{(t)}$ and $\mathbf{x}_j^{(t)}$ for which $\|\mathbf{x}_i^{(t)} - \mathbf{x}_j^{(t)}\| < \delta$. For such a pair, tentatively merge them into their midpoint $(\mathbf{x}_i^{(t)} + \mathbf{x}_j^{(t)})/2$ with combined weight $w_i^{(t)} + w_j^{(t)}$, and denote the resulting design as $\boldsymbol{\xi}_{\text{mer}}$. If $|\mathbf{F}(\boldsymbol{\xi}_{\text{mer}})| > 0$, replace the two design points with their merged one and reduce m_t by 1; otherwise, do not merge them. Stop if all such pairs have been examined.

Step 3: Given $\boldsymbol{\xi}_t \in \Xi$ after the merging step, apply the lift-one algorithm with the convergence threshold ϵ , and obtain an EW D-optimal allocation $(w_1^*, \dots, w_{m_t}^*)^T$ for the design points $\{\mathbf{x}_1^{(t)}, \dots, \mathbf{x}_{m_t}^{(t)}\}$. Replace $w_i^{(t)}$ with w_i^* , respectively.

Step 4: Deleting step: Update $\boldsymbol{\xi}_t$ by discarding any $\mathbf{x}_i^{(t)}$ for which $w_i^{(t)} = 0$.

Step 5: Adding new point: Given $\boldsymbol{\xi}_t \in \Xi$, find $\mathbf{x}^* = (x_1^*, \dots, x_d^*)^T \in \mathcal{X}$ that maximizes $d(\mathbf{x}, \boldsymbol{\xi}_t)$. More specifically, if all factors are continuous, \mathbf{x}^* can be obtained by the ‘‘L-BFGS-B’’ quasi-Newton method (Byrd et al., 1995) directly. If the first k factors are continuous with $1 \leq k \leq d - 1$, then we may first find

$$\mathbf{x}_{(1)}^* = \arg\max_{\mathbf{x}_{(1)} \in \prod_{j=1}^k [a_j, b_j]} d((\mathbf{x}_{(1)}^T, \mathbf{x}_{(2)}^T)^T, \boldsymbol{\xi}_t)$$

for each $\mathbf{x}_{(2)} = (x_{k+1}, \dots, x_d)^T \in \prod_{j=k+1}^d I_j$, and then choose $\mathbf{x}_{(2)}^*$ that yields the largest $d((\mathbf{x}_{(1)}^*)^T, \mathbf{x}_{(2)}^T, \boldsymbol{\xi}_t)$. Note that $\mathbf{x}_{(1)}^*$ depends on $\mathbf{x}_{(2)}$. Then $\mathbf{x}^* = ((\mathbf{x}_{(1)}^*)^T, (\mathbf{x}_{(2)}^*)^T)^T$.

Step 6: If $d(\mathbf{x}^*, \boldsymbol{\xi}_t) \leq p$, proceed to Step 7. Otherwise, obtain $\boldsymbol{\xi}_{t+1}$ by adding $(\mathbf{x}^*, 0)$ to $\boldsymbol{\xi}_t$ and increasing m_t by 1, and return to Step 2.

Step 7: Output $\boldsymbol{\xi}_t$ as an EW D-optimal design.

Note that the EW ForLion algorithm is essentially applying the original ForLion algorithm proposed by Huang et al. (2024) to $\mathbf{F}(\boldsymbol{\xi})$ under an EW D-optimality. It should be noted that Step 2 in Algorithm 1 is different from the merging step in the original ForLion algorithm by addressing a possible issue when the merging step leads to a degenerated $\mathbf{F}(\boldsymbol{\xi}_{\text{mer}})$, which is possible in practice.

According to Step 6 in Algorithm 1, $\boldsymbol{\xi}_t$ reported by the EW ForLion algorithm satisfies $\max_{\mathbf{x} \in \mathcal{X}} d(\mathbf{x}, \boldsymbol{\xi}_t) \leq p$. As a direct conclusion of Theorem 2.1, we have the following corollary.

Corollary 3.1. *For sample-based EW D-optimality under Assumptions (A1), (A2), and (B3), or integral-based EW D-optimality under Assumptions (A1), (A3), and (B3), the design obtained by Algorithm 1 must be EW D-optimal.*

Since the design found by Algorithm 1 is an approximate design with continuous design points, to facilitate practical uses, we propose a rounding algorithm (see Algorithm 2) to convert an approximate design to an exact design with user-specified set of grid points.

Algorithm 2: **Rounding Algorithm**

Step 0: Input: An approximate design $\boldsymbol{\xi} = \{(\mathbf{x}_i, w_i), i = 1, \dots, m_0\} \in \Xi$ with all $w_i > 0$ and $|\mathbf{F}(\boldsymbol{\xi})| > 0$, a pre-specified merging threshold δ_r (e.g., $\delta_r = 0.1$, typically larger than δ in Algorithm 1), grid levels (or pace lengths) L_1, \dots, L_k for the k continuous factors (e.g., $L_1 = \dots = L_k = 0.25$), respectively, and the total number n of experimental units.

Step 1: Merging step: For each pair of \mathbf{x}_i and \mathbf{x}_j , define their distance $d_{ij} = \|\mathbf{x}_i - \mathbf{x}_j\|$ if their levels of discrete factors are identical; and ∞ otherwise. If $d_{ij} < \delta_r$, tentatively merge \mathbf{x}_i and \mathbf{x}_j into a single design point $(w_i \mathbf{x}_i + w_j \mathbf{x}_j) / (w_i + w_j)$ with combined weight $w_i + w_j$, and denote the resulting design as $\boldsymbol{\xi}_{\text{mer}}$. If $|\mathbf{F}(\boldsymbol{\xi}_{\text{mer}})| > 0$, replace $\boldsymbol{\xi}$ with $\boldsymbol{\xi}_{\text{mer}}$; otherwise, do not merge. Stop if all such pairs have been examined.

Step 2: Rounding design points to grid levels: Round the continuous components of each design point to their nearest multiples of the corresponding L_j , $j = 1, \dots, k$.

Step 3: Allocating experimental units: First set $n_i = \lfloor n w_i \rfloor$, the largest integer no more than $n w_i$, and then allocate any remaining units to design points with $n w_i > n_i$, in the order of increasing $\mathbf{F}(\boldsymbol{\xi})$ the most (see Algorithm 2 in Huang et al. (2025)).

Step 4: Deleting step: Discard any \mathbf{x}_i for which $n_i = 0$.

Step 5: Output: Exact design $\{(\mathbf{x}_i, n_i), i = 1, \dots, m\}$ with $n_i > 0$ and $\sum_{i=1}^m n_i = n$.

3.3 Calculating $E\{\mathbf{F}(\mathbf{x}, \boldsymbol{\Theta})\}$ or $\hat{E}\{\mathbf{F}(\mathbf{x}, \boldsymbol{\Theta})\}$

To implement the EW ForLion algorithm (Algorithm 1) for EW D-optimal designs, it is critical to calculate $E\{\mathbf{F}(\mathbf{x}, \boldsymbol{\Theta})\}$ or $\hat{E}\{\mathbf{F}(\mathbf{x}, \boldsymbol{\Theta})\}$ efficiently.

Example 3.1. Multinomial logistic models (MLM): For MLMs (Glonck and McCullagh, 1995; Zocchi and Atkinson, 1999; Bu et al., 2020), according to Theorem 2 of Huang et al. (2024)), it is enough to replace $u_{st}^{\mathbf{x}}$, or $u_{st}^{\mathbf{x}}(\boldsymbol{\theta})$ as it is a function of $\boldsymbol{\theta}$, with $E\{u_{st}^{\mathbf{x}}(\boldsymbol{\Theta})\} = \int_{\Theta} u_{st}^{\mathbf{x}}(\boldsymbol{\theta})Q(d\boldsymbol{\theta})$ or $\hat{E}\{u_{st}^{\mathbf{x}}(\boldsymbol{\Theta})\} = B^{-1} \sum_{j=1}^B u_{st}^{\mathbf{x}}(\hat{\boldsymbol{\theta}}_j)$, for $s, t = 1, \dots, J$. The formulae for calculating $u_{st}^{\mathbf{x}}$ as a function of $\boldsymbol{\theta}$ can be found in Appendix A in Huang et al. (2024).

An alternative way is to utilize Corollary 3.1 in Bu et al. (2020). In our notation, $\mathbf{F}(\mathbf{x}, \boldsymbol{\theta}) = \mathbf{X}_{\mathbf{x}}^T \mathbf{U}_{\mathbf{x}}(\boldsymbol{\theta}) \mathbf{X}_{\mathbf{x}}$, where

$$\mathbf{X}_{\mathbf{x}} = \begin{pmatrix} \mathbf{h}_1^T(\mathbf{x}) & \mathbf{0}^T & \dots & \mathbf{0}^T & \mathbf{h}_c^T(\mathbf{x}) \\ \mathbf{0}^T & \mathbf{h}_2^T(\mathbf{x}) & \ddots & \vdots & \vdots \\ \vdots & \ddots & \ddots & \mathbf{0}^T & \mathbf{h}_c^T(\mathbf{x}) \\ \mathbf{0}^T & \dots & \mathbf{0}^T & \mathbf{h}_{J-1}^T(\mathbf{x}) & \mathbf{h}_c^T(\mathbf{x}) \\ \mathbf{0}^T & \dots & \dots & \mathbf{0}^T & \mathbf{0}^T \end{pmatrix}_{J \times p} \quad (5)$$

with pre-determined predictor functions $\mathbf{h}_j = (h_{j1}, \dots, h_{jp_j})^T$, $j = 1, \dots, J-1$, $\mathbf{h}_c = (h_1, \dots, h_{p_c})^T$, and $\mathbf{U}_{\mathbf{x}}(\boldsymbol{\theta}) = (u_{st}^{\mathbf{x}}(\boldsymbol{\theta}))_{s,t=1,\dots,J}$. Then $E\{\mathbf{F}(\mathbf{x}, \boldsymbol{\Theta})\} = \mathbf{X}_{\mathbf{x}}^T E\{\mathbf{U}_{\mathbf{x}}(\boldsymbol{\Theta})\} \mathbf{X}_{\mathbf{x}}$ and $\hat{E}\{\mathbf{F}(\mathbf{x}, \boldsymbol{\Theta})\} = \mathbf{X}_{\mathbf{x}}^T \hat{E}\{\mathbf{U}_{\mathbf{x}}(\boldsymbol{\Theta})\} \mathbf{X}_{\mathbf{x}}$. \square

Theorem 3.1. *For MLMs under Assumptions (A1) and (B3), suppose all the predictor functions $\mathbf{h}_1, \dots, \mathbf{h}_{J-1}$ and \mathbf{h}_c defined in (5) are continuous with respect to all continuous factors of $\mathbf{x} \in \mathcal{X}$, and the parameter space $\Theta \subseteq \mathbb{R}^p$ is bounded. Then there exists an EW D-optimal design $\boldsymbol{\xi}$ that contains no more than $p(p+1)/2$ support points, and the design obtained by Algorithm 1 must be EW D-optimal.*

The boundedness of Θ in Theorem 3.1 is a practical requirement. For typical applications, the boundedness of a working parameter space is often needed for a numerical search for parameter estimates or a theoretical derivation for desired properties (Ferguson, 1996).

Example 3.2. Generalized linear models (GLM): For a generalized linear model (McCullagh and Nelder, 1989; Dobson and Barnett, 2018) defined by

$$E(Y_i) = \mu_i \text{ and } \eta_i = g(\mu_i) = \mathbf{X}_i^T \boldsymbol{\theta},$$

where g is a given link function, $\mathbf{X}_i = \mathbf{h}(\mathbf{x}_i) = (h_1(\mathbf{x}_i), \dots, h_p(\mathbf{x}_i))^T$, $i = 1, \dots, m$ (see, for example, Section 4 in Huang et al. (2024)). Then $\mathbf{F}(\mathbf{x}, \boldsymbol{\theta}) = \nu\{\mathbf{h}(\mathbf{x})^T \boldsymbol{\theta}\} \cdot \mathbf{h}(\mathbf{x})\mathbf{h}(\mathbf{x})^T$, where $\nu = \{(g^{-1})'\}^2/s$ with $s(\eta_i) = \text{Var}(Y_i)$ (see Table 5 in the Supplementary Material of Huang et al. (2025) for examples of ν). To calculate $E\{\mathbf{F}(\mathbf{x}, \boldsymbol{\Theta})\}$ or $\hat{E}\{\mathbf{F}(\mathbf{x}, \boldsymbol{\Theta})\}$ under GLMs, it is enough to replace $\nu\{\mathbf{h}(\mathbf{x})^T \boldsymbol{\theta}\}$ with $E[\nu\{\mathbf{h}(\mathbf{x})^T \boldsymbol{\Theta}\}] = \int_{\Theta} \nu\{\mathbf{h}(\mathbf{x})^T \boldsymbol{\theta}\}Q(d\boldsymbol{\theta})$ or $\hat{E}[\nu\{\mathbf{h}(\mathbf{x})^T \boldsymbol{\Theta}\}] = B^{-1} \sum_{j=1}^B \nu\{\mathbf{h}(\mathbf{x})^T \hat{\boldsymbol{\theta}}_j\}$. That is, $E\{\mathbf{F}(\mathbf{x}, \boldsymbol{\Theta})\} = E[\nu\{\mathbf{h}(\mathbf{x})^T \boldsymbol{\Theta}\}] \cdot \mathbf{h}(\mathbf{x})\mathbf{h}(\mathbf{x})^T$, and $\hat{E}\{\mathbf{F}(\mathbf{x}, \boldsymbol{\Theta})\} = \hat{E}[\nu\{\mathbf{h}(\mathbf{x})^T \boldsymbol{\Theta}\}] \cdot \mathbf{h}(\mathbf{x})\mathbf{h}(\mathbf{x})^T$.

To calculate $\mathbf{F}(\boldsymbol{\xi}, \boldsymbol{\theta})$ under GLMs, instead of using $\sum_{i=1}^m w_i \mathbf{F}(\mathbf{x}_i, \boldsymbol{\theta})$, one may use its matrix form $\mathbf{F}(\boldsymbol{\xi}, \boldsymbol{\theta}) = \mathbf{X}_{\boldsymbol{\xi}}^T \mathbf{W}_{\boldsymbol{\xi}}(\boldsymbol{\theta}) \mathbf{X}_{\boldsymbol{\xi}}$, where $\mathbf{X}_{\boldsymbol{\xi}} = (\mathbf{h}(\mathbf{x}_1), \dots, \mathbf{h}(\mathbf{x}_m))^T \in \mathbb{R}^{m \times p}$, and $\mathbf{W}_{\boldsymbol{\xi}}(\boldsymbol{\theta}) = \text{diag}\{w_1 \nu\{\mathbf{h}(\mathbf{x}_1)^T \boldsymbol{\theta}\}, \dots, w_m \nu\{\mathbf{h}(\mathbf{x}_m)^T \boldsymbol{\theta}\}\}$. Then, under a GLM,

$$E\{\mathbf{F}(\boldsymbol{\xi}, \boldsymbol{\Theta})\} = \mathbf{X}_{\boldsymbol{\xi}}^T E\{\mathbf{W}_{\boldsymbol{\xi}}(\boldsymbol{\Theta})\} \mathbf{X}_{\boldsymbol{\xi}} \text{ and } \hat{E}\{\mathbf{F}(\boldsymbol{\xi}, \boldsymbol{\Theta})\} = \mathbf{X}_{\boldsymbol{\xi}}^T \hat{E}\{\mathbf{W}_{\boldsymbol{\xi}}(\boldsymbol{\Theta})\} \mathbf{X}_{\boldsymbol{\xi}}.$$

Note that the matrix form is much more efficient especially when programming in R. \square

Theorem 3.2. *For GLMs under Assumptions (A1) and (B3), suppose all the predictor functions $\mathbf{h} = (h_1, \dots, h_p)^T$ are continuous with respect to all continuous factors of $\mathbf{x} \in \mathcal{X}$, and Θ is bounded. Then there exists an EW D-optimal design ξ that contains no more than $p(p+1)/2$ support points, and the design obtained by Algorithm 1 must be EW D-optimal.*

4. Applications to Real Experiments

In this section, we use the paper feeder experiment (see Section 1) and a minimizing surface defects experiment, both under MLMs, to illustrate the advantages gained by adopting our algorithms and the EW D-optimal designs. For examples under GLMs, please see Section S7 of the Supplementary Material.

4.1 Paper feeder experiment

In this section, we consider the motivating example mentioned in Section 1, the paper feeder experiment. There are eight discrete control factors and one continuous factor, the stack force, under our consideration (see Section S5 for more details). As mentioned in Section 1, instead of using two separate GLMs to model the two types of failures, **misfeed** and **multifeed**, we consider multinomial logistic models (MLM) to model all three possible outcomes, namely **misfeed**, **normal**, and **multifeed**, at the same time. Using Akaike information criterion (AIC, Akaike (1973)) and Bayesian information criterion (BIC, Hastie et al. (2009)), we adopt a cumulative logit model with npo as the most appropriate model for this experiment (see Table S.1 in Section S5 of the Supplementary Material).

For this experiment, we compare ten different designs (see Tables 1 and 2): (1) “Original allocation”: the original design that collected 1,785 observations roughly uniformly at 183 distinct experimental settings; (2) “EW Bu-appro”: an approximate design obtained by applying Bu et al. (2020)’s EW lift-one algorithm on the original 183 distinct settings; (3) “EW Bu-exact”: an exact design obtained by applying Bu et al. (2020)’s EW exchange algorithm on the 183 distinct settings with $n = 1,785$; (4) “EW Bu-grid2.5” & (5) “EW Bu-grid2.5 exact”: approximate and exact designs by applying Bu et al. (2020)’s algorithms after discretizing the stack force factor in $[0, 160]$ into grid points with equal space 2.5; (6) “EW ForLion”: the proposed EW D-optimal approximate design by applying our EW ForLion algorithm to the continuous factor in $[0, 160]$; (7)~(10) exact designs obtained by applying Algorithm 2 with different grid levels or pace lengths ($L = 0.1, 0.5, 1, 2.5$) and $n = 1,785$. For illustration purpose, all designs follow the same 18 runs modified from $OA(18, 2^1 \times 2^7)$ for the eight discrete factors, while their design points can be different in terms of the continuous factor. Since the feasible space of a cumulative logit model is not rectangular (see Example 5.2 in Bu et al. (2020) or Example 8 in Huang et al. (2025)), we bootstrap the original dataset to collect $B = 100$ (due to computational intensity) samples and the corresponding estimated model parameters, denoted by $\hat{\theta}_1, \hat{\theta}_2, \dots, \hat{\theta}_{100}$. All the EW designs are under the sample-based EW D-optimality with respect to the 100 parameter vectors. The constructed designs are

presented in Tables S.3 and S.4 of the Supplementary Material.

In Table 1, we list the number of design points m , the computational time in seconds for obtaining the designs, the objective function values, and the relative efficiencies compared with the recommended EW ForLion design, that is, $(|\hat{E}\{\mathbf{F}(\boldsymbol{\xi}, \boldsymbol{\Theta})\}|/|\hat{E}\{\mathbf{F}(\boldsymbol{\xi}_{\text{ForLion}}, \boldsymbol{\Theta})\}|)^{1/p}$ with $p = 32$. Compared with our EW ForLion design, the original design on 183 settings only attains 63.03% relative efficiency. Having applied Bu et al. (2020)’s algorithms on the same 183 settings, the relative efficiencies of EW Bu-appro and EW Bu-exact, 88.16% and 88.15%, are not satisfactory either. When we apply Bu et al. (2020)’s algorithms on grid points with length 2.5, it takes much longer time to find EW Bu-grid2.5 and EW Bu-grid2.5 exact designs, which also need more settings (55 and 44). The EW ForLion design and its exact designs at different grid levels require the minimum number of experimental settings, shorter computational time, and higher relative efficiencies.

Table 1: Robust designs for the paper feeder experiment

Designs	m	Time (s)	$ \hat{E}\{\mathbf{F}(\boldsymbol{\xi}, \boldsymbol{\theta})\} $	Relative Efficiency
Original allocation	183	-	1.342e+28	63.03%
EW Bu-appro	38	116s	6.162e+32	88.16%
EW Bu-exact	38	1095s	6.159e+32	88.15%
EW Bu-grid2.5	55	15201s	2.078e+34	98.40%
EW Bu-grid2.5 exact	44	69907s	2.078e+34	98.40%
EW ForLion	38	1853s	3.482e+34	100.00%
EW ForLion exact grid0.1	38	0.28s	2.122e+34	98.46%
EW ForLion exact grid0.5	38	0.24s	2.065e+34	98.38%
EW ForLion exact grid1	38	0.23s	1.579e+34	97.56%
EW ForLion exact grid2.5	38	0.22s	1.326e+34	97.03%

Note: Time for EW ForLion exact designs are for applying Algorithm 2 to EW ForLion (approximate) design.

To assess the robustness of these designs, we first use the original ForLion algorithm (Huang et al., 2024) to find the corresponding locally D-optimal design $\boldsymbol{\xi}_j^*$ for each $\hat{\boldsymbol{\theta}}_j$. Then the robustness of a design $\boldsymbol{\xi} \in \Xi$ can be evaluated by the 100 relative efficiencies $(|\mathbf{F}(\boldsymbol{\xi}, \hat{\boldsymbol{\theta}}_j)|/|\mathbf{F}(\boldsymbol{\xi}_j^*, \hat{\boldsymbol{\theta}}_j)|)^{1/p}$, $j = 1, \dots, 100$. Table 2 (see also Figure S.2 in the Supplementary Material) presents the five-number summary of the 100 relative efficiencies. Overall, the EW ForLion design is the most robust one against parameter misspecifications. For practical uses, we recommend the grid-0.1 exact design (EW ForLion exact grid0.1), which has nearly the same robustness as the EW D-optimal approximate design and the smallest number of distinct experimental settings (i.e., 38).

4.2 Minimizing surface defects

Wu (2008) presented a study that investigated optimal parameter settings in a polysilicon deposition process for circuit manufacturing. This experiment involves responses of five categories, five continuous control factors, and one discrete control factor (see Table S1 in the Supplementary Material of Huang et al. (2024) or Table 6 in Lukemire et al. (2022)). Lukemire et al. (2022) employed a PSO algorithm and derived a locally D-optimal approximate design with 14 support points under a cumulative logit model with

Table 2: Relative efficiencies w.r.t. locally D-optimal designs for paper feeder experiment

Robust design	Min	Q_1	Median	Q_3	Max
Original allocation	0.5075	0.6005	0.6115	0.6308	0.6587
EW Bu-appro	0.6813	0.8133	0.8343	0.8488	0.8741
EW Bu-exact	0.6813	0.8134	0.8346	0.8489	0.8742
EW Bu-grid2.5	0.7592	0.9183	0.9327	0.9417	0.9513
EW Bu-grid2.5 exact	0.7594	0.9184	0.9328	0.9417	0.9515
EW ForLion	0.8363	0.9277	0.9364	0.9445	0.9542
EW ForLion exact grid0.1	0.8028	0.9276	0.9361	0.9443	0.9541
EW ForLion exact grid0.5	0.7569	0.9269	0.9363	0.9447	0.9534
EW ForLion exact grid1	0.7502	0.9163	0.9315	0.9389	0.9489
EW ForLion exact grid2.5	0.7548	0.9098	0.9253	0.9348	0.9439

po, while Huang et al. (2024) applied their ForLion algorithm and obtained a locally D-optimal approximate design with 17 design points.

In practice, an experimenter may not know the precise nominal values for some or all parameters but often has varying degrees of insight into their actual values. To construct a robust design against parameter misspecifications, we sample $B = 1000$ parameter vectors from the prior distributions listed in Table S1 of the Supplementary Material of Huang et al. (2024) for the cumulative logit model with po as follows:

$$\log \left(\frac{\pi_{i1} + \dots + \pi_{ij}}{\pi_{i,j+1} + \dots + \pi_{iJ}} \right) = \theta_j - \beta_1 x_{i1} - \beta_2 x_{i2} - \beta_3 x_{i3} - \beta_4 x_{i4} - \beta_5 x_{i5} - \beta_6 x_{i6}$$

with $i = 1, \dots, m$, $j = 1, 2, 3, 4$, and $J = 5$, where $\pi_{ij} \in (0, 1)$ stands for the probability that the response associated with $\mathbf{x}_i = (x_{i1}, \dots, x_{i6})^T$ falls into the j th category.

We use Algorithm 1 to construct a sample-based EW D-optimal approximate design (see the left side of Table 3). Assuming that the total number of experimental units is $n = 1000$, we apply our Algorithm 2 with $L_1 = \dots = L_5 = 1$ for continuous control variables and obtain an exact design, as shown on the right side of Table 3. Both our approximate and exact designs have 17 support points.

To compare our EW ForLion D-optimal designs with Bu et al. (2020)’s EW D-optimal designs constructed on grid points, we discretize each of the five continuous control factors into 2 or 4 evenly distributed grid points, which leads to $2 \times 2^5 = 64$ or $2 \times 4^5 = 2,048$ possible design points, respectively. Discretizations with higher number of grid points are skipped due to computational intensity. Then Bu et al. (2020)’s lift-one algorithm is applied to the discretized design region and the corresponding EW D-optimal approximate designs are constructed (EW Bu grid2 and EW Bu grid4 in Figure 1).

To compare the robustness of different designs against parameter misspecifications, we sample 10,000 parameter vectors from the prior distribution provided in Table S1 of Huang et al. (2024). For each sampled parameter vector $\boldsymbol{\theta}_j$, we calculate the relative efficiency of a design $\boldsymbol{\xi}$ under comparison with respect to our EW ForLion approximate design $\boldsymbol{\xi}_{\text{EWForLion}}$, i.e., $(|\mathbf{F}(\boldsymbol{\xi}, \boldsymbol{\theta}_j)|/|\mathbf{F}(\boldsymbol{\xi}_{\text{EWForLion}}, \boldsymbol{\theta}_j)|)^{1/p}$ with $p = 10$ in this case.

Figure 1 shows histograms and boxplots of 10,000 relative efficiencies for Bu et al. (2020)’s EW D-optimal designs on grid-2 or grid-4 design regions, EW ForLion exact design by applying our Algorithm 2 to the EW ForLion approximate design, and locally D-optimal designs obtained by Huang et al. (2024)’s original ForLion algorithm or

Table 3: EW D-optimal approximate (left) and exact (right) designs by EW ForLion and rounding algorithms for minimizing surface defects experiment

Design point	Cleaning Method	Temp.	Pressure	Nit.Flow	Sil.Flow	Time	w_i	Design point	Cleaning Method	Temp.	Pressure	Nit.Flow	Sil.Flow	Time	n_i
1	-1	-25.000	200.000	-150	0	0	0.0475	1	-1	-25	200	-150	0	0	48
2	1	25.000	0	0	0	0	0.0986	2	1	25	0	0	0	0	99
3	1	25.000	200.000	-150	0	16	0.0380	3	1	25	200	-150	0	16	38
4	-1	-25.000	0	0	0	16	0.1206	4	-1	-25	0	0	0	16	121
5	1	0	0	0	0	16	0.0984	5	1	0	0	0	0	16	98
6	-1	25.000	-104.910	-150	-100	16	0.0426	6	-1	25	-105	-150	-100	16	43
7	-1	14.870	-1.299	0	0	0	0.1017	7	-1	15	-1	0	0	0	102
8	1	-13.168	2.802	0	0	16	0.0399	8	1	-13	3	0	0	16	40
9	-1	25.000	111.805	0	-100	16	0.0533	9	-1	25	112	0	-100	16	53
10	-1	25.000	-72.107	0	-100	16	0.0432	10	-1	25	-72	0	-100	16	43
11	-1	-25.000	-170.690	-150	0	0	0.0401	11	-1	-25	-171	-150	0	0	40
12	1	25.000	-158.631	-150	0	16	0.0470	12	1	25	-159	-150	0	16	47
13	1	-25.000	-200.000	-150	-100	0	0.0215	13	1	-25	-200	-150	-100	0	21
14	1	-25.000	-20.500	0	-100	0	0.0843	14	1	-25	-20	0	-100	0	84
15	1	-25.000	200.000	-150	-100	0	0.0415	15	1	-25	200	-150	-100	0	42
16	1	-2.925	0.017	0	0	0	0.0294	16	1	-3	0	0	0	0	29
17	-1	-10.568	-1.093	0	0	0	0.0524	17	-1	-11	-1	0	0	0	52

Lukemire et al. (2022)’s PSO. It is evident that the EW ForLion exact design performs very similar to the EW ForLion approximate design. In most cases, the original ForLion and PSO designs yield relative efficiencies less than 1. EW Bu grid4 design performs apparently better than EW Bu grid2, but not as good as EW ForLion designs. Overall we recommend our EW ForLion approximate and exact designs.

5. Conclusion

In this paper, we characterize EW D-optimal designs for fairly general parametric models with mixed factors and derive detailed formulae for multinomial logistic models and generalized linear models. We develop an EW ForLion algorithm for finding EW D-optimal designs with mixed factors or continuous factors, and a rounding algorithm to convert approximate designs to exact designs.

Depending on the availability of a pilot study or a prior distribution on unknown parameters, we recommend either sample-based or integral-based EW D-optimal designs. Apparently, the obtained EW D-optimal design depends on the set of parameter vectors or the prior distribution chosen. By applying our algorithms to real experiments, we show that the obtained EW D-optimal designs under a reasonable parameter vector set or prior distribution provide well-performed robust designs against parameter misspecifications. By merging close design settings, our designs may significantly reduce the design cost and time by minimizing the number of distinct design settings.

References

- Abramowitz, M., and Stegun, I. A. (1970), *Handbook of Mathematical Functions with Formulas, Graphs, and Mathematical Tables*, Dover Publications, 9th ed.
- Ai, M., Ye, Z., and Yu, J. (2023), “Locally D-Optimal Designs for Hierarchical Response Experiments,” *Statistica Sinica*, 33, 381–399.
- Akaike, H. (1973), in *Proceedings of the 2nd International Symposium on Information Theory*, eds. Petrov, B., and Csaki, F., Akademiai Kiado, Budapest, pp. 267–281.

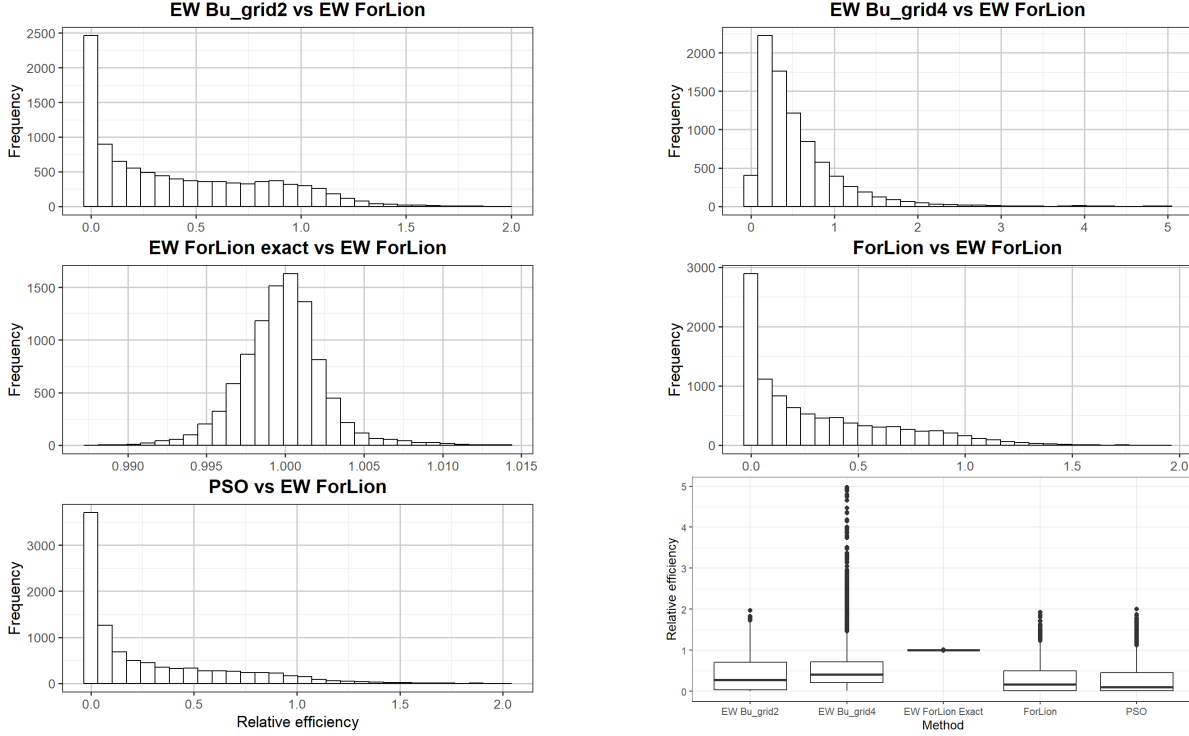


Figure 1: Relative efficiency comparison among designs for 10000 sampled parameter sets in the minimizing surface defects experiment

Atkinson, A. C., Donev, A. N., and Tobias, R. D. (2007), *Optimum Experimental Designs, with SAS*, Oxford, United Kingdom: Oxford University Press.

Billingsley, P. (1999), *Convergence of Probability Measures*, John Wiley & Sons, 2nd ed.

Bu, X., Majumdar, D., and Yang, J. (2020), “D-optimal Designs for Multinomial Logistic Models,” *Annals of Statistics*, 48, 983–1000.

Byrd, R. H., Lu, P., Nocedal, J., and Zhu, C. (1995), “A limited memory algorithm for bound constrained optimization,” *SIAM Journal on scientific computing*, 16, 1190–1208.

Chaloner, K., and Verdinelli, I. (1995), “Bayesian experimental design: a review,” *Statistical Science*, 10, 273–304.

Chernoff, H. (1953), “Locally optimal designs for estimating parameters,” *Annals of Mathematical Statistics*, 24, 586–602.

Dobson, A., and Barnett, A. (2018), *An Introduction to Generalized Linear Models*, Chapman & Hall/CRC, 4th ed.

Fedorov, V. (1972), *Theory of Optimal Experiments*, Academic Press.

Fedorov, V., and Leonov, S. (2014), *Optimal Design for Nonlinear Response Models*, Chapman & Hall/CRC.

- Fedorov, V. V., and Hackl, P. (1997), *Model-Oriented Design of Experiments*, Springer Science & Business Media.
- Ferguson, T. (1996), *A Course in Large Sample Theory*, Chapman & Hall.
- Glonek, G., and McCullagh, P. (1995), “Multivariate logistic models,” *Journal of the Royal Statistical Society, Series B*, 57, 533–546.
- Harman, R., Filová, L., and Richtárik, P. (2020), “A randomized exchange algorithm for computing optimal approximate designs of experiments,” *Journal of the American Statistical Association*, 115, 348–361.
- Hastie, T., Tibshirani, R., and Friedman, J. (2009), *The Elements of Statistical Learning: Data Mining, Inference, and Prediction*, Springer, 2nd ed.
- Huang, Y., Li, K., Mandal, A., and Yang, J. (2024), “ForLion: A New Algorithm for D-optimal Designs under General Parametric Statistical Models with Mixed Factors,” *Statistics and Computing*, 34, 157.
- Huang, Y., Tong, L., and Yang, J. (2025), “Constrained D-optimal design for paid research study,” *Statistica Sinica*, to appear, available at https://www3.stat.sinica.edu.tw/ss_newpaper/SS-2022-0414_na.pdf.
- Joseph, V., and Wu, C. (2004), “Failure amplification method: an information maximization approach to categorical response optimization (with discussions),” *Technometrics*, 46, 1–31.
- Kennedy, J., and Eberhart, R. (1995), “Particle swarm optimization,” in *Proceedings of ICNN’95-International Conference on Neural Networks*, IEEE, vol. 4, pp. 1942–1948.
- Kiefer, J. (1974), “General equivalence theory for optimum designs (approximate theory),” *Annals of Statistics*, 2, 849–879.
- Lehmann, E. L., and Casella, G. (1998), *Theory of Point Estimation*, Springer, New York, 2nd ed.
- Lukemire, J., Mandal, A., and Wong, W. K. (2019), “d-QPSO: A quantum-behaved particle swarm technique for finding D-optimal designs with discrete and continuous factors and a binary response,” *Technometrics*, 61, 77–87.
- Lukemire, J., Mandal, A., and Wong, W. K. (2022), “Optimal experimental designs for ordinal models with mixed factors for industrial and healthcare applications,” *Journal of Quality Technology*, 54, 184–196.
- McCullagh, P., and Nelder, J. (1989), *Generalized Linear Models*, Chapman and Hall/CRC, 2nd ed.
- Poli, R., Kennedy, J., and Blackwell, T. (2007), “Particle swarm optimization: An overview,” *Swarm Intelligence*, 1, 33–57.

- Pukelsheim, F. (1993), *Optimal Design of Experiments*, John Wiley & Sons.
- Resnick, S. (2003), *A Probability Path*, Springer Science & Business Media.
- Silvey, S., Titterington, D., and Torsney, B. (1978), “An algorithm for optimal designs on a finite design space,” *Communications in Statistics - Theory and Methods*, 14, 1379–1389.
- Stufken, J., and Yang, M. (2012), *Optimal designs for generalized linear models*, Wiley, chap. 4, pp. 137–164.
- Titterington, D. (1976), “Algorithms for computing D-optimal design on finite design spaces,” in *Proc. of the 1976 Conf. on Information Science and Systems*, John Hopkins University, vol. 3, pp. 213–216.
- (1978), “Estimation of correlation coefficients by ellipsoidal trimming,” *Journal of the Royal Statistical Society, Series C (Applied Statistics)*, 27, 227–234.
- Tong, L., Volkmer, H., and Yang, J. (2014), “Analytic solutions for D-optimal factorial designs under generalized linear models,” *Electronic Journal of Statistics*, 8, 1322–1344.
- Wu, C., and Hamada, M. (2009), *Experiments: Planning, Analysis, and Optimization*, Wiley, 2nd ed.
- Wu, F.-C. (2008), “Simultaneous optimization of robust design with quantitative and ordinal data,” *International Journal of Industrial Engineering: Theory, Applications and Practice*, 5, 231–238.
- Yang, J., and Mandal, A. (2015), “D-optimal factorial designs under generalized linear models,” *Communications in Statistics - Simulation and Computation*, 44, 2264–2277.
- Yang, J., Mandal, A., and Majumdar, D. (2016), “Optimal designs for 2^k factorial experiments with binary response,” *Statistica Sinica*, 26, 385–411.
- Yang, J., Tong, L., and Mandal, A. (2017), “D-optimal designs with ordered categorical data,” *Statistica Sinica*, 27, 1879–1902.
- Yang, M., Biedermann, S., and Tang, E. (2013), “On optimal designs for nonlinear models: a general and efficient algorithm,” *Journal of the American Statistical Association*, 108, 1411–1420.
- Yu, Y. (2010), “Monotonic convergence of a general algorithm for computing optimal designs,” *Annals of Statistics*, 38, 1593–1606.
- Zocchi, S., and Atkinson, A. (1999), “Optimum experimental designs for multinomial logistic models,” *Biometrics*, 55, 437–444.

EW D-optimal Designs for Experiments with Mixed Factors

Siting Lin¹, Yifei Huang², and Jie Yang¹

¹University of Illinois at Chicago and ²Astellas Pharma, Inc.

Supplementary Material

- S1 Analytic Solutions for Multinomial Logistic Models
- S2 Assumptions and Relevant Results
- S3 First-order Derivative of Sensitivity Function
- S4 Proofs of Main Theorems
- S5 Model Selection and Design Comparison for Paper Feeder Experiment
- S6 Robustness of Sample-based EW Designs
- S7 More Examples

S1. Analytic Solutions for Multinomial Logistic Models

According to Theorem S.9 in the Supplementary Material of Bu et al. (2020), for multinomial logistic models, given a design $\xi = \{(\mathbf{x}_i, w_i) \mid i = 1, \dots, m\} \in \Xi$, for $i \in \{1, \dots, m\}$ and $0 < z < 1$, we have

$$\begin{aligned} f_i(z) &= (1-z)^{p-J+1} \sum_{j=0}^{J-1} b_j z^j (1-z)^{J-1-j}, \\ f'_i(z) &= (1-z)^{p-J} \sum_{j=1}^{J-1} b_j (j-pz) z^{j-1} (1-z)^{J-1-j} - p b_0 (1-z)^{p-1}, \end{aligned}$$

where $b_0 = f_i(0)$, $(b_{J-1}, b_{J-2}, \dots, b_1)^T = \mathbf{B}_{J-1}^{-1} \mathbf{c}$, $\mathbf{B}_{J-1} = (s^{t-1})_{s,t=1,2,\dots,J-1}$, and $\mathbf{c} = (c_1, c_2, \dots, c_{J-1})^T$ with $c_j = (j+1)^p j^{J-1-p} f_i(1/(j+1)) - j^{J-1} f_i(0)$, $j = 1, \dots, J-1$.

For typically applications, $p \geq J \geq 3$. Since $f_i(z)$ is an order- p polynomial in z with $f_i(1) = 0$, its maximum on $[0, 1]$ is attained either at $z = 0$ or at an interior point $z \in (0, 1)$ satisfying $f'_i(z) = 0$, that is,

$$\sum_{j=1}^{J-1} j b_j z^{j-1} (1-z)^{J-j-1} = p \sum_{j=0}^{J-1} b_j z^j (1-z)^{J-j-1}, \quad 0 < z < 1. \quad (\text{S.1})$$

In Bu et al. (2020), it was mentioned that (S.1) has analytic solutions for $J \leq 5$, while no formula was provided accordingly. In this section, we provide explicit solutions to facilitate the programming for multinomial logistic models. Note that we only need the real-valued solutions locating in $(0, 1)$ for our purposes.

According to the analytic solutions to quadratic, cubic, and quartic equations (see, for example, Sections 3.8.1~3.8.3 in Abramowitz and Stegun (1970)), we have the following results:

Lemma S1.1. *When $J = 3$, (S.1) can be rewritten as $A_2 z^2 + A_1 z + A_0 = 0$ with $A_2 = p(b_0 - b_1 + b_2)$, $A_1 = b_1(1+p) - 2(b_0 p + b_2)$, and $A_0 = b_0 p - b_1$.*

- (i) *If $A_2 = A_1 = A_0 = 0$, then (S.1) has infinitely many solutions in $(0, 1)$ and $f_i(z) \equiv f_i(0) \geq 0$. In this case, we may choose $z = 0$ to maximize $f_i(z)$.*

(ii) If $A_2 = A_1 = 0$ but $A_0 \neq 0$, then we must have $A_0 > 0$. In this case, (S.1) has no solution, while $z = 0$ uniquely maximizes $f_i(z)$ with $z \in [0, 1]$.

(iii) If $A_2 = 0$ but $A_1 \neq 0$, then (S.1) has a unique solution $-A_0/A_1 \in \mathbb{R}$.

(iv) If $A_2 \neq 0$ and $A_1^2 - 4A_2A_0 > 0$, then (S.1) has two real solutions

$$\frac{-A_1 \pm \sqrt{A_1^2 - 4A_2A_0}}{2A_2}.$$

(v) If $A_2 \neq 0$ and $A_1^2 - 4A_2A_0 = 0$, then (S.1) has only one real solution $-A_1/(2A_2)$.

(vi) If $A_2 \neq 0$ and $A_1^2 - 4A_2A_0 < 0$, then (S.1) has no real solution.

Proof of Lemma S1.1: When $J = 3$, (S.1) can be rewritten as $A_2z^2 + A_1z + A_0 = 0$ with $A_2 = p(b_0 - b_1 + b_2)$, $A_1 = b_1(1 + p) - 2(b_0p + b_2)$, $A_0 = b_0p - b_1$, and

$$f'_i(z) = -(1 - z)^{p-J}(A_2z^2 + A_1z + A_0).$$

We only need to verify case (ii). Actually, in this case, if $A_0 < 0$, then $f'_i(z) = -(1 - z)^{p-J}A_0 > 0$ for all $z \in (0, 1)$, while $f_i(0) \geq 0 = f_i(1)$ leads to a contradiction. \square

As a direct conclusion of Sections 3.8.2 in Abramowitz and Stegun (1970), we obtain the following lemma for $J = 4$:

Lemma S1.2. When $J = 4$, equation (S.1) is equivalent to $A_3z^3 + A_2z^2 + A_1z + A_0 = 0$ with $A_0 = b_0p - b_1$, $A_1 = -3b_0p + b_1(2 + p) - 2b_2$, $A_2 = 3b_0p - b_1(1 + 2p) + b_2(2 + p) - 3b_3$, and $A_3 = p(-b_0 + b_1 - b_2 + b_3)$. The cases with $A_3 = 0$ has been listed in Lemma S1.1. If $A_3 \neq 0$, (S.1) is equivalent to $z^3 + a_2z^2 + a_1z + a_0 = 0$ with $a_i = A_i/A_3$, $i = 0, 1, 2$. We let

$$q = \frac{a_1}{3} - \frac{a_2^2}{9}, \quad r = \frac{a_1a_2 - 3a_0}{6} - \frac{a_2^3}{27},$$

$$s_1 = [r + (q^3 + r^2)^{1/2}]^{1/3}, \text{ and } s_2 = [r - (q^3 + r^2)^{1/2}]^{1/3}.$$

(i) If $q^3 + r^2 > 0$, then (S.1) has only one real solution $s_1 + s_2 - a_2/3$.

(ii) If $q^3 + r^2 = 0$, then (S.1) has two real solutions $z_1 = 2r^{1/3} - a_2/3$ and $z_2 = -r^{1/3} - a_2/3$.

(iii) If $q^3 + r^2 < 0$, then (S.1) has three real solutions

$$z_1 = s_1 + s_2 - \frac{a_2}{3}, \quad z_2, z_3 = -\frac{s_1 + s_2}{2} - \frac{a_2}{3} \pm \frac{i\sqrt{3}}{2}(s_1 - s_2)$$

with $i = \sqrt{-1}$, known as the imaginary unit.

For $J = 5$, we follow the arguments for equation (12) in Tong et al. (2014) and obtain the following results:

Lemma S1.3. When $J = 5$, equation (S.1) is equivalent to $A_4z^4 + A_3z^3 + A_2z^2 + A_1z + A_0 = 0$ with $A_0 = b_0p - b_1$, $A_1 = -4b_0p + b_1(3 + p) - 2b_2$, $A_2 = 6b_0p - 3b_1(1 + p) + b_2(4 + p) - 3b_3$, and $A_3 = -4b_0p + b_1(1 + 3p) - 2b_2(1 + p) + b_3(3 + p) - 4b_4$, and $A_4 = p(b_0 - b_1 + b_2 - b_3 + b_4)$. The cases with $A_4 = 0$ has been listed in Lemmas S1.2 & S1.1. If $A_4 \neq 0$, (S.1) is equivalent to $z^4 + a_3z^3 + a_2z^2 + a_1z + a_0 = 0$ with $a_i = A_i/A_4$, $i = 0, 1, 2, 3$. Then there are four solutions to (S.1) calculated as complex numbers:

$$z_1, z_2 = -\frac{a_3}{4} - \frac{\sqrt{A_*}}{2} \pm \frac{\sqrt{B_*}}{2}, \quad z_3, z_4 = -\frac{a_3}{4} + \frac{\sqrt{A_*}}{2} \pm \frac{\sqrt{C_*}}{2}$$

with

$$\begin{aligned}
A_* &= -\frac{2a_2}{3} + \frac{a_3^2}{4} + \frac{G_*}{3 \times 2^{1/3}}, \\
B_* &= -\frac{4a_2}{3} + \frac{a_3^2}{2} - \frac{G_*}{3 \times 2^{1/3}} - \frac{-8a_1 + 4a_2a_3 - a_3^3}{4\sqrt{A_*}}, \\
C_* &= -\frac{4a_2}{3} + \frac{a_3^2}{2} - \frac{G_*}{3 \times 2^{1/3}} + \frac{-8a_1 + 4a_2a_3 - a_3^3}{4\sqrt{A_*}}, \\
D_* &= \left(F_* + \sqrt{F_*^2 - 4E_*^3}\right)^{1/3}, \\
E_* &= 12a_0 + a_2^2 - 3a_1a_3, \\
F_* &= 27a_1^2 - 72a_0a_2 + 2a_2^3 - 9a_1a_2a_3 + 27a_0a_3^2, \\
G_* &= D_* + 2^{2/3}E_*/D_*.
\end{aligned}$$

S2. Assumptions and Relevant Results

Following Fedorov and Leonov (2014) and Huang et al. (2024), in this section we list the assumptions needed for this paper. Note that our assumptions have been adjusted for mixed factors. Recall that a design point or experimental setting $\mathbf{x} = (x_1, \dots, x_d)^T \in \mathcal{X} \subseteq \mathbb{R}^d$. Among the $d \geq 1$ factors, the first k factors are continuous, and the last $d - k$ factors are discrete. Note that $0 \leq k \leq d$ and $k = 0$ implies no continuous factor. When $k \geq 1$, we denote $\mathbf{x}_1 = (x_1, \dots, x_k)^T$ as the vector of continuous factors.

- (A1) The design region $\mathcal{X} \subset \mathbb{R}^d$ is compact.
(In this paper, $\mathcal{X} = \prod_{j=1}^d I_j$, where $I_j = [a_j, b_j]$ with $-\infty < a_j < b_j < \infty$ for continuous factors, and $I_j = \{c_{j1}, \dots, c_{jm_j}\}$ with $-\infty < a_j = c_{j1} < \dots < c_{jm_j} = b_j < \infty$ and $m_j \geq 2$ for discrete factors.)
- (A2) For each $\boldsymbol{\theta} \in \boldsymbol{\Theta}$, if $k \geq 1$, the Fisher information $\mathbf{F}(\mathbf{x}, \boldsymbol{\theta})$ is element-wise continuous with respect to all continuous factors of $\mathbf{x} \in \mathcal{X}$.
- (A3) For each $\boldsymbol{\theta} \in \boldsymbol{\Theta}$, if $k \geq 1$, the Fisher information $\mathbf{F}(\mathbf{x}, \boldsymbol{\theta}) = (F_{st}(\mathbf{x}, \boldsymbol{\theta}))_{s,t=1,\dots,p}$ is element-wise continuous with respect to all continuous factors of $\mathbf{x} \in \mathcal{X}$, and there exists a nonnegative and integrable function $K(\boldsymbol{\theta})$ on $\boldsymbol{\Theta}$, such that, $\int_{\boldsymbol{\Theta}} K(\boldsymbol{\theta}) Q(d\boldsymbol{\theta}) < \infty$, and $|F_{st}(\mathbf{x}, \boldsymbol{\theta})| \leq K(\boldsymbol{\theta})$, for all $s, t \in \{1, \dots, p\}$, $\mathbf{x} \in \mathcal{X}$, and $\boldsymbol{\theta} \in \boldsymbol{\Theta}$.

Note that (i) if $k = 0$, that is, all factors are discrete, then both Assumption (A2) and the first half (i.e., the continuous statement) of Assumption (A3) are automatically satisfied; (ii) when $k \geq 1$, that is, there is at least one continuous factor, (A3) always implies (A2).

Lemma S2.1. Suppose $k \geq 1$ and the parametric model $M(\mathbf{x}, \boldsymbol{\theta})$ with $\mathbf{x} \in \mathcal{X}$ and $\boldsymbol{\theta} \in \boldsymbol{\Theta}$ satisfies Assumption (A2). Given $\{\hat{\boldsymbol{\theta}}_1, \dots, \hat{\boldsymbol{\theta}}_B\} \subseteq \boldsymbol{\Theta}$, $\hat{E}\{\mathbf{F}(\mathbf{x}, \boldsymbol{\Theta})\} = \frac{1}{B} \sum_{j=1}^B \mathbf{F}(\mathbf{x}, \hat{\boldsymbol{\theta}}_j)$ is element-wise continuous with respect to all continuous factors of $\mathbf{x} \in \mathcal{X}$.

The proof of Lemma S2.1 is straightforward. It is for sample-based EW designs. For integral-based EW designs, we need the following lemma:

Lemma S2.2. Suppose $k \geq 1$ and the parametric model $M(\mathbf{x}, \boldsymbol{\theta})$ with $\mathbf{x} \in \mathcal{X}$ and $\boldsymbol{\theta} \in \boldsymbol{\Theta}$ satisfies Assumption (A3). Then $E\{\mathbf{F}(\mathbf{x}, \boldsymbol{\theta})\} = \int_{\boldsymbol{\Theta}} \mathbf{F}(\mathbf{x}, \boldsymbol{\theta}) Q(d\boldsymbol{\theta})$ is element-wise continuous with respect to all continuous factors of $\mathbf{x} \in \mathcal{X}$.

Proof of Lemma S2.2. Given any $\mathbf{x}_0 = (x_{01}, \dots, x_{0d})^T \in \mathcal{X}$, we let $\{\mathbf{x}_n = (x_{n1}, \dots, x_{nd})^T \in \mathcal{X} \mid n \geq 1\}$ be a sequence of design points, such that, $\lim_{n \rightarrow \infty} \mathbf{x}_n = \mathbf{x}_0$. If $k < d$, then we must have $(x_{n,k+1}, \dots, x_{nd}) \equiv (x_{0,k+1}, \dots, x_{0d})$ for large enough n .

For any $s, t \in \{1, \dots, p\}$, since $F_{st}(\mathbf{x}, \boldsymbol{\theta})$ is continuous with respect to $\mathbf{x}_1 = (x_1, \dots, x_k)^T$, we must have $\lim_{n \rightarrow \infty} F_{st}(\mathbf{x}_n, \boldsymbol{\theta}) = F_{st}(\mathbf{x}_0, \boldsymbol{\theta})$ for each $\boldsymbol{\theta} \in \boldsymbol{\Theta}$. Since (A3) is satisfied, according to the Dominated Convergence Theorem (see, for example, Theorem 5.3.3 in Resnick (2003)), we must have

$$\lim_{n \rightarrow \infty} E\{F_{st}(\mathbf{x}_n, \boldsymbol{\Theta})\} = \lim_{n \rightarrow \infty} \int_{\boldsymbol{\Theta}} F_{st}(\mathbf{x}_n, \boldsymbol{\theta}) Q(d\boldsymbol{\theta}) = \int_{\boldsymbol{\Theta}} F_{st}(\mathbf{x}_0, \boldsymbol{\theta}) Q(d\boldsymbol{\theta}) = E\{F_{st}(\mathbf{x}_0, \boldsymbol{\Theta})\}$$

for each $\mathbf{x}_0 \in \mathcal{X}$, as long as $\lim_{n \rightarrow \infty} \mathbf{x}_n = \mathbf{x}_0$. That is, $E\{\mathbf{F}(\mathbf{x}, \boldsymbol{\Theta})\}$ is element-wise continuous with respect to \mathbf{x}_1 . \square

Following Fedorov and Leonov (2014), to characterize the sample-based and integral-based D-optimal EW designs, we extend the collection Ξ of designs (each design consists of only a finite number of design points) to $\Xi(\mathcal{X})$, which consists of all probability measures on \mathcal{X} . In other words, a design $\xi \in \Xi(\mathcal{X})$ is also a probability measure on \mathcal{X} , and for each $\theta \in \Theta$,

$$\mathbf{F}(\xi, \theta) = \int_{\mathcal{X}} \mathbf{F}(\mathbf{x}, \theta) \xi(d\mathbf{x}) .$$

Then for sample-based EW criterion, we denote

$$\mathbf{F}_{\text{SEW}}(\xi) = \hat{E}\{\mathbf{F}(\xi, \Theta)\} = \frac{1}{B} \sum_{j=1}^B \mathbf{F}(\xi, \hat{\theta}_j) = \int_{\mathcal{X}} \hat{E}\{\mathbf{F}(\mathbf{x}, \Theta)\} \xi(d\mathbf{x}) . \quad (\text{S.2})$$

For integral-based EW criterion, under Assumption (A3) and Fubini Theorem (see, for example, Theorem 5.9.2 in Resnick (2003)), we denote

$$\begin{aligned} \mathbf{F}_{\text{EW}}(\xi) &= E\{\mathbf{F}(\xi, \Theta)\} = \int_{\Theta} \mathbf{F}(\xi, \theta) Q(d\theta) \\ &= \int_{\Theta} \int_{\mathcal{X}} \mathbf{F}(\mathbf{x}, \theta) \xi(d\mathbf{x}) Q(d\theta) \\ &= \int_{\mathcal{X}} \int_{\Theta} \mathbf{F}(\mathbf{x}, \theta) Q(d\theta) \xi(d\mathbf{x}) \quad (\text{by Fubini Theorem}) \\ &= \int_{\mathcal{X}} E\{\mathbf{F}(\mathbf{x}, \Theta)\} \xi(d\mathbf{x}) . \end{aligned} \quad (\text{S.3})$$

Since the Fisher information matrices $\mathbf{F}(\mathbf{x}, \hat{\theta}_j)$ and $\mathbf{F}(\mathbf{x}, \theta)$ are symmetric and nonnegative definite for all $\mathbf{x} \in \mathcal{X}$ and $\hat{\theta}_j, \theta \in \Theta$, and both integration and convex combination preserve symmetry and nonnegative definiteness, then $\mathbf{F}(\xi, \theta)$, $\mathbf{F}(\xi, \hat{\theta}_j)$, $\mathbf{F}_{\text{SEW}}(\xi)$, and $\mathbf{F}_{\text{EW}}(\xi)$ are symmetric and nonnegative definite as well.

Following Fedorov and Leonov (2014), we further denote the corresponding collections of Fisher information matrices:

$$\begin{aligned} \mathcal{F}_{\text{SEW}}(\mathcal{X}) &= \{\mathbf{F}_{\text{SEW}}(\xi) \mid \xi \in \Xi(\mathcal{X})\} , \\ \mathcal{F}_{\text{EW}}(\mathcal{X}) &= \{\mathbf{F}_{\text{EW}}(\xi) \mid \xi \in \Xi(\mathcal{X})\} . \end{aligned}$$

For any $\theta \in \Theta$, $\mathbf{F}(\xi, \theta)$ is linear in $\xi \in \Xi(\mathcal{X})$. Actually, for any two designs $\xi_1, \xi_2 \in \Xi(\mathcal{X})$ and any $\lambda \in [0, 1]$, it can be verified that

$$\mathbf{F}(\lambda \xi_1 + (1 - \lambda) \xi_2, \theta) = \lambda \mathbf{F}(\xi_1, \theta) + (1 - \lambda) \mathbf{F}(\xi_2, \theta) ,$$

which further implies

$$\begin{aligned} \mathbf{F}_{\text{SEW}}(\lambda \xi_1 + (1 - \lambda) \xi_2) &= \lambda \mathbf{F}_{\text{SEW}}(\xi_1) + (1 - \lambda) \mathbf{F}_{\text{SEW}}(\xi_2) , \\ \mathbf{F}_{\text{EW}}(\lambda \xi_1 + (1 - \lambda) \xi_2) &= \lambda \mathbf{F}_{\text{EW}}(\xi_1) + (1 - \lambda) \mathbf{F}_{\text{EW}}(\xi_2) . \end{aligned}$$

That is, both $\mathcal{F}_{\text{SEW}}(\mathcal{X})$ and $\mathcal{F}_{\text{EW}}(\mathcal{X})$ are convex.

Since \mathcal{X} is compact under Assumption (A1), it can be verified that $\Xi(\mathcal{X})$ is also compact under the topology of weak convergence, that is, ξ_n converges weakly to ξ_0 , as n goes to ∞ , if and only if $\lim_{n \rightarrow \infty} \int_{\mathcal{X}} f(\mathbf{x}) \xi_n(d\mathbf{x}) = \int_{\mathcal{X}} f(\mathbf{x}) \xi_0(d\mathbf{x})$ for all bounded continuous function f on \mathcal{X} (Billingsley, 1999; Fedorov and Leonov, 2014). Further with Assumption (A2), $\hat{E}\{\mathbf{F}(\mathbf{x}, \Theta)\}$ is element-wise continuous with respect to all continuous factors of $\mathbf{x} \in \mathcal{X}$ due to Lemma S2.1, and must be bounded due to the compactness of \mathcal{X} , then \mathbf{F}_{SEW} as a map from $\Xi(\mathcal{X})$ to $\mathbb{R}^{p \times p}$ is also bounded continuous, and thus its image $\mathcal{F}_{\text{SEW}}(\mathcal{X})$ is also compact. Similarly with Assumption (A3) and Lemma S2.2, \mathbf{F}_{EW} is a bounded continuous map from $\Xi(\mathcal{X})$ to $\mathbb{R}^{p \times p}$, and $\mathcal{F}_{\text{EW}}(\mathcal{X})$ is compact as well.

As a summary, we have the following lemma:

Lemma S2.3. *Under Assumptions (A1) and (A2), $\mathcal{F}_{\text{SEW}}(\mathcal{X})$ is convex and compact; under Assumptions (A1) and (A3), $\mathcal{F}_{\text{EW}}(\mathcal{X})$ is convex and compact as well.*

Theorem S2.1. *If Assumptions (A1) and (A2) hold, then for any $p \times p$ matrix $\mathbf{F} \in \mathcal{F}_{\text{SEW}}(\mathcal{X})$, there exists a design $\xi \in \Xi \subset \Xi(\mathcal{X})$ with no more than $m = p(p+1)/2 + 1$ points, such that $\mathbf{F}_{\text{SEW}}(\xi) = \mathbf{F}$. If \mathbf{F} is a boundary point of the convex set $\mathcal{F}_{\text{SEW}}(\mathcal{X})$, then we need no more than $p(p+1)/2$ support points for ξ . If Assumptions (A1) and (A3) are satisfied, then the same conclusions hold for $\mathcal{F}_{\text{EW}}(\mathcal{X})$ and $\mathbf{F}_{\text{EW}}(\xi)$ as well.*

Proof of Theorem S2.1. Under Assumptions (A1) and (A2), following the proof of the lemma in Section 1.26 of Pukelsheim (1993), it can be verified that $\{\mathbf{F}_{\text{SEW}}(\boldsymbol{\xi}) \mid \boldsymbol{\xi} \in \Xi\} \subset \mathbb{R}^{p \times p}$, as the convex hull of the set $\{\hat{E}\{\mathbf{F}(\mathbf{x}, \boldsymbol{\Theta})\} \mid \mathbf{x} \in \mathcal{X}\}$ with dimension $p(p+1)/2$ due to their symmetry, is convex and compact. Due to Lemma S2.3 and Carathéodory's Theorem (see, for example, Theorem 2.1.1 in Fedorov (1972)), it can be further verified that for any matrix $\mathbf{F} \in \mathcal{F}_{\text{SEW}}(\mathcal{X})$ with $\boldsymbol{\xi} \in \Xi(\mathcal{X})$, there exists a $\boldsymbol{\xi}_0 \in \Xi$ with at most $p(p+1)/2 + 1$ design points, such that, $\mathbf{F}_{\text{SEW}}(\boldsymbol{\xi}_0) = \mathbf{F}$. When $\mathbf{F} \in \mathcal{F}_{\text{SEW}}(\mathcal{X})$ is a boundary point (that is, any open set of $\mathcal{F}_{\text{SEW}}(\mathcal{X})$ containing \mathbf{F} contains both matrices inside and outside $\mathcal{F}_{\text{SEW}}(\mathcal{X})$), the number of design points in $\boldsymbol{\xi}_0$ can be at most $p(p+1)/2$.

Similarly, we can obtain the same conclusions for $\{\mathbf{F}_{\text{EW}}(\boldsymbol{\xi}) \mid \boldsymbol{\xi} \in \Xi\}$, $\{E\{\mathbf{F}(\mathbf{x}, \boldsymbol{\Theta})\} \mid \mathbf{x} \in \mathcal{X}\}$, and $\mathcal{F}_{\text{EW}}(\mathcal{X})$ under Assumptions (A1) and (A3). \square

To characterize D-optimality for EW designs, we define the objective function

$$\Psi(\mathbf{F}) = -\log |\mathbf{F}|$$

for $\mathbf{F} \in \mathcal{F}_{\text{SEW}}(\mathcal{X})$ or $\mathcal{F}_{\text{EW}}(\mathcal{X})$. Then $f_{\text{SEW}}(\boldsymbol{\xi}) = \exp\{-\Psi(\hat{E}\{\mathbf{F}(\boldsymbol{\xi}, \boldsymbol{\Theta})\})\}$, and $f_{\text{EW}}(\boldsymbol{\xi}) = \exp\{-\Psi(E\{\mathbf{F}(\boldsymbol{\xi}, \boldsymbol{\Theta})\})\}$. Note that minimizing $\Psi(\mathbf{F})$ for $\mathbf{F} \in \mathcal{F}_{\text{SEW}}(\mathcal{X})$ or $\mathcal{F}_{\text{EW}}(\mathcal{X})$ is equivalent to maximizing $f_{\text{SEW}}(\boldsymbol{\xi})$ or $f_{\text{EW}}(\boldsymbol{\xi})$ for $\boldsymbol{\xi} \in \Xi$, respectively, due to Theorem S2.1.

According to Section 2.4.2 in Fedorov and Leonov (2014), for D-optimality, Ψ always satisfies their Assumptions (B1), (B2), and (B4). In our notations, we let $\Xi(q)$ denote $\{\boldsymbol{\xi} \in \Xi \mid |\hat{E}\{\mathbf{F}(\boldsymbol{\xi}, \boldsymbol{\Theta})\}| \geq q\}$ for sample-based EW D-optimality, or $\{\boldsymbol{\xi} \in \Xi \mid |E\{\mathbf{F}(\boldsymbol{\xi}, \boldsymbol{\Theta})\}| \geq q\}$ for integral-based EW D-optimality. We also denote $\mathbf{F}(\boldsymbol{\xi}) = \hat{E}\{\mathbf{F}(\boldsymbol{\xi}, \boldsymbol{\Theta})\}$ for sample-based EW D-optimality, and $\mathbf{F}(\boldsymbol{\xi}) = E\{\mathbf{F}(\boldsymbol{\xi}, \boldsymbol{\Theta})\}$ for integral-based EW D-optimality. Similarly, $\mathbf{F}_{\mathbf{x}} = \hat{E}\{\mathbf{F}(\mathbf{x}, \boldsymbol{\Theta})\}$ for sample-based EW D-optimality, and $\mathbf{F}_{\mathbf{x}} = E\{\mathbf{F}(\mathbf{x}, \boldsymbol{\Theta})\}$ for integral-based EW D-optimality. Then the corresponding assumptions are provided as below.

(B1) $\Psi(\mathbf{F})$ is a convex function for $\mathbf{F} \in \mathcal{F}_{\text{SEW}}(\mathcal{X})$ or $\mathcal{F}_{\text{EW}}(\mathcal{X})$.

(B2) $\Psi(\mathbf{F})$ is a monotonically non-increasing function for $\mathbf{F} \in \mathcal{F}_{\text{SEW}}(\mathcal{X})$ or $\mathcal{F}_{\text{EW}}(\mathcal{X})$.

(B3) There exists a $q > 0$, such that $\Xi(q)$ is non-empty.

(B4) For any $\boldsymbol{\xi} \in \Xi(q)$, $\bar{\boldsymbol{\xi}} \in \Xi$, and $\alpha \in (0, 1)$,

$$\Psi[(1-\alpha)\mathbf{F}(\boldsymbol{\xi}) + \alpha\mathbf{F}(\bar{\boldsymbol{\xi}})] = \Psi[\mathbf{F}(\boldsymbol{\xi})] + \alpha \int_{\mathcal{X}} \psi(\mathbf{x}, \boldsymbol{\xi}) \bar{\boldsymbol{\xi}}(d\mathbf{x}) + o(\alpha),$$

as $\alpha \rightarrow 0$, where $\psi(\mathbf{x}, \boldsymbol{\xi}) = p - \text{tr}[\mathbf{F}(\boldsymbol{\xi})^{-1}\mathbf{F}_{\mathbf{x}}]$.

S3. First-order Derivative of Sensitivity Function

To implement the EW ForLion algorithm (Algorithm 1) for EW D-optimal designs, if there is at least one continuous factor, we need to calculate the first-order derivative of the sensitivity function $d(\mathbf{x}, \boldsymbol{\xi})$ (Huang et al., 2024).

Following the simplified notation in Section 3.2, we denote

$$\begin{aligned} \mathbf{F}(\boldsymbol{\xi}) &= \begin{cases} E\{\mathbf{F}(\boldsymbol{\xi}, \boldsymbol{\Theta})\} & \text{, under integral-based EW D-optimality;} \\ \hat{E}\{\mathbf{F}(\boldsymbol{\xi}, \boldsymbol{\Theta})\} & \text{, under sample-based EW D-optimality,} \end{cases} \\ \mathbf{F}_{\mathbf{x}} &= \begin{cases} E\{\mathbf{F}(\mathbf{x}, \boldsymbol{\Theta})\} & \text{, under integral-based EW D-optimality;} \\ \hat{E}\{\mathbf{F}(\mathbf{x}, \boldsymbol{\Theta})\} & \text{, under sample-based EW D-optimality,} \end{cases} \end{aligned}$$

Then $d(\mathbf{x}, \boldsymbol{\xi})$ in Theorem 2.1 can be simplified to $d(\mathbf{x}, \boldsymbol{\xi}) = \text{tr}(\mathbf{F}(\boldsymbol{\xi})^{-1}\mathbf{F}_{\mathbf{x}})$.

Similar to Theorem 3 in Huang et al. (2024), we obtain the following theorem for multinomial logistic models (MLM) under EW D-optimality.

Theorem S3.1. For an MLM model under Assumptions (A1) and (B3), consider $\boldsymbol{\xi} \in \Xi$ satisfying $|\mathbf{F}(\boldsymbol{\xi})| > 0$. If we denote the $p \times p$ matrix

$$\mathbf{F}(\boldsymbol{\xi})^{-1} = \begin{bmatrix} \mathbf{E}_{11} & \cdots & \mathbf{E}_{1J} \\ \vdots & \ddots & \vdots \\ \mathbf{E}_{J1} & \cdots & \mathbf{E}_{JJ} \end{bmatrix}$$

with submatrix $\mathbf{E}_{st} \in \mathbf{R}^{p_s \times p_t}$ (we denote $p_J = p_c$ for simplicity), then

$$\begin{aligned} d(\mathbf{x}, \boldsymbol{\xi}) &= \text{tr}(\mathbf{F}(\boldsymbol{\xi})^{-1} \mathbf{F}_{\mathbf{x}}) \\ &= \sum_{t=1}^{J-1} u_{tt}^{\mathbf{x}} (\mathbf{h}_t^{\mathbf{x}})^T \mathbf{E}_{tt} \mathbf{h}_t^{\mathbf{x}} + \sum_{s=1}^{J-1} \sum_{t=1}^{J-1} u_{st}^{\mathbf{x}} (\mathbf{h}_c^{\mathbf{x}})^T \mathbf{E}_{sJ} \mathbf{h}_c^{\mathbf{x}} \\ &\quad + 2 \sum_{s=1}^{J-2} \sum_{t=s+1}^{J-1} u_{st}^{\mathbf{x}} (\mathbf{h}_t^{\mathbf{x}})^T \mathbf{E}_{st} \mathbf{h}_s^{\mathbf{x}} + 2 \sum_{s=1}^{J-1} \sum_{t=1}^{J-1} u_{st}^{\mathbf{x}} (\mathbf{h}_c^{\mathbf{x}})^T \mathbf{E}_{sJ} \mathbf{h}_s^{\mathbf{x}}, \end{aligned}$$

with $\mathbf{h}_j^{\mathbf{x}} = \mathbf{h}_j(\mathbf{x})$, $\mathbf{h}_c^{\mathbf{x}} = \mathbf{h}_c(\mathbf{x})$, and

$$u_{st}^{\mathbf{x}} = \begin{cases} E\{u_{st}^{\mathbf{x}}(\boldsymbol{\Theta})\} & , \text{ under integral-based EW D-optimality;} \\ \hat{E}\{u_{st}^{\mathbf{x}}(\boldsymbol{\Theta})\} & , \text{ under sample-based EW D-optimality,} \end{cases}$$

as in Example 3.1 for simplicity.

Example S3.1. Multinomial logistic models (MLM): To calculate the first-order derivative of $d(\mathbf{x}, \boldsymbol{\xi})$ under MLMs, we follow Appendix C in Huang et al. (2024) after

- (i) $\mathbf{F}(\boldsymbol{\xi})$ is replaced with $E\{\mathbf{F}(\boldsymbol{\xi}, \boldsymbol{\Theta})\}$ or $\hat{E}\{\mathbf{F}(\boldsymbol{\xi}, \boldsymbol{\Theta})\}$ for each $\boldsymbol{\xi} \in \Xi$;
- (ii) $\mathbf{F}_{\mathbf{x}}$ is replaced with $E\{\mathbf{F}(\mathbf{x}, \boldsymbol{\Theta})\}$ or $\hat{E}\{\mathbf{F}(\mathbf{x}, \boldsymbol{\Theta})\}$ for each $\mathbf{x} \in \mathcal{X}$;
- (iii) $\mathbf{U}_{\mathbf{x}} = (u_{st}^{\mathbf{x}})_{s,t=1,\dots,J}$ is replaced by $(E\{u_{st}^{\mathbf{x}}(\boldsymbol{\Theta})\})_{s,t=1,\dots,J}$ or $(\hat{E}\{u_{st}^{\mathbf{x}}(\boldsymbol{\Theta})\})_{s,t=1,\dots,J}$ (see also Example 3.1);
- (iv) If $k \geq 1$, for $i = 1, \dots, k$, $\frac{\partial \mathbf{U}_{\mathbf{x}}}{\partial x_i} = \left(\frac{\partial u_{st}^{\mathbf{x}}}{\partial x_i} \right)_{s,t=1,\dots,J}$ is replaced by

$$\left(\frac{\partial E\{u_{st}^{\mathbf{x}}(\boldsymbol{\Theta})\}}{\partial x_i} \right)_{s,t=1,\dots,J} = \left(\frac{\partial}{\partial x_i} \int_{\boldsymbol{\Theta}} u_{st}^{\mathbf{x}}(\boldsymbol{\theta}) Q(d\boldsymbol{\theta}) \right)_{s,t=1,\dots,J}$$

or

$$\left(\hat{E} \left\{ \frac{\partial u_{st}^{\mathbf{x}}}{\partial x_i}(\boldsymbol{\Theta}) \right\} \right)_{s,t=1,\dots,J} = \left(\frac{1}{B} \sum_{j=1}^B \frac{\partial u_{st}^{\mathbf{x}}}{\partial x_i}(\hat{\boldsymbol{\theta}}_j) \right)_{s,t=1,\dots,J}. \quad (\text{S.4})$$

Note that $\frac{\partial u_{st}^{\mathbf{x}}}{\partial x_i}(\hat{\boldsymbol{\theta}}_j)$ in (S.4) denotes $\frac{\partial u_{st}^{\mathbf{x}}}{\partial x_i}$ at $\boldsymbol{\theta} = \hat{\boldsymbol{\theta}}_j$. One can use the formulae in Appendix C of Huang et al. (2024) to calculate it for each $j = 1, \dots, B$. \square

Example S3.2. Generalized linear models (GLM): Under GLMs, the sensitivity function

$$d(\mathbf{x}, \boldsymbol{\xi}) = E[\nu\{\mathbf{h}(\mathbf{x})^T \boldsymbol{\Theta}\}] \cdot \mathbf{h}(\mathbf{x})^T [E\{\mathbf{F}(\boldsymbol{\xi}, \boldsymbol{\Theta})\}]^{-1} \mathbf{h}(\mathbf{x}) \quad (\text{S.5})$$

for $f_{\text{EW}}(\boldsymbol{\xi})$ or

$$d(\mathbf{x}, \boldsymbol{\xi}) = \hat{E}[\nu\{\mathbf{h}(\mathbf{x})^T \boldsymbol{\Theta}\}] \cdot \mathbf{h}(\mathbf{x})^T \left[\hat{E}\{\mathbf{F}(\boldsymbol{\xi}, \boldsymbol{\Theta})\} \right]^{-1} \mathbf{h}(\mathbf{x}) \quad (\text{S.6})$$

for $f_{\text{SEW}}(\boldsymbol{\xi})$. Following the notation in Section S.5 of the Supplementary Material of Huang et al. (2024), we denote $\mathbf{A}_E = [\mathbf{X}_{\boldsymbol{\xi}}^T E\{\mathbf{W}_{\boldsymbol{\xi}}(\boldsymbol{\Theta})\} \mathbf{X}_{\boldsymbol{\xi}}]^{-1}$ and $\mathbf{A}_{\hat{E}} = [\mathbf{X}_{\boldsymbol{\xi}}^T \hat{E}\{\mathbf{W}_{\boldsymbol{\xi}}(\boldsymbol{\Theta})\} \mathbf{X}_{\boldsymbol{\xi}}]^{-1}$. The first-order derivative of $d(\mathbf{x}, \boldsymbol{\xi})$ with respect to continuous factors $\mathbf{x}_{(1)} = (x_1, \dots, x_k)^T$ is

$$\frac{\partial d(\mathbf{x}, \boldsymbol{\xi})}{\partial \mathbf{x}_{(1)}} = \mathbf{h}(\mathbf{x})^T \mathbf{A}_E \mathbf{h}(\mathbf{x}) \cdot \frac{\partial E[\nu\{\mathbf{h}(\mathbf{x})^T \boldsymbol{\Theta}\}]}{\partial \mathbf{x}_{(1)}} + 2 \cdot E[\nu\{\mathbf{h}(\mathbf{x})^T \boldsymbol{\Theta}\}] \cdot \left\{ \frac{\partial \mathbf{h}(\mathbf{x})}{\partial \mathbf{x}_{(1)}^T} \right\}^T \mathbf{A}_E \mathbf{h}(\mathbf{x})$$

for $f_{EW}(\xi)$, or

$$\begin{aligned}
\frac{\partial d(\mathbf{x}, \xi)}{\partial \mathbf{x}_{(1)}} &= \mathbf{h}(\mathbf{x})^T \mathbf{A}_{\hat{E}} \mathbf{h}(\mathbf{x}) \cdot \frac{\partial \hat{E}[\nu\{\mathbf{h}(\mathbf{x})^T \boldsymbol{\Theta}\}]}{\partial \mathbf{x}_{(1)}} + 2 \cdot \hat{E}[\nu\{\mathbf{h}(\mathbf{x})^T \boldsymbol{\Theta}\}] \cdot \left\{ \frac{\partial \mathbf{h}(\mathbf{x})}{\partial \mathbf{x}_{(1)}^T} \right\}^T \mathbf{A}_{\hat{E}} \mathbf{h}(\mathbf{x}) \\
&= \mathbf{h}(\mathbf{x})^T \mathbf{A}_{\hat{E}} \mathbf{h}(\mathbf{x}) \cdot \left\{ \frac{\partial \mathbf{h}(\mathbf{x})}{\partial \mathbf{x}_{(1)}^T} \right\}^T \cdot \frac{1}{B} \sum_{j=1}^B \nu' \{\mathbf{h}(\mathbf{x})^T \hat{\boldsymbol{\theta}}_j\} \hat{\boldsymbol{\theta}}_j \\
&\quad + \frac{2}{B} \cdot \sum_{j=1}^B \nu \{\mathbf{h}(\mathbf{x})^T \hat{\boldsymbol{\theta}}_j\} \cdot \left\{ \frac{\partial \mathbf{h}(\mathbf{x})}{\partial \mathbf{x}_{(1)}^T} \right\}^T \mathbf{A}_{\hat{E}} \mathbf{h}(\mathbf{x})
\end{aligned}$$

for $f_{SEW}(\xi)$. \square

Similar to Theorem 4 in Huang et al. (2024), we obtain the following result for GLM under EW D-optimality.

Theorem S3.2. *For a GLM model under Assumptions (A1) and (B3), consider $\xi \in \Xi$ satisfying $|\mathbf{X}_{\xi}^T \mathbf{W}_{\xi} \mathbf{X}_{\xi}| > 0$, where \mathbf{W}_{ξ} is either $E\{\mathbf{W}_{\xi}(\boldsymbol{\Theta})\}$ for integral-based EW D-optimality or $\hat{E}\{\mathbf{W}_{\xi}(\boldsymbol{\Theta})\}$ for sample-based EW D-optimality (see Example 3.2). Then ξ is EW D-optimal if and only if $\max_{\mathbf{x} \in \mathcal{X}} E[\nu\{\mathbf{h}(\mathbf{x})^T \boldsymbol{\Theta}\}] \cdot \mathbf{h}(\mathbf{x})^T [\mathbf{X}_{\xi}^T \mathbf{W}_{\xi} \mathbf{X}_{\xi}]^{-1} \cdot \mathbf{h}(\mathbf{x}) \leq p$ for integral-based D-optimality or $\max_{\mathbf{x} \in \mathcal{X}} \hat{E}[\nu\{\mathbf{h}(\mathbf{x})^T \boldsymbol{\Theta}\}] \cdot \mathbf{h}(\mathbf{x})^T [\mathbf{X}_{\xi}^T \mathbf{W}_{\xi} \mathbf{X}_{\xi}]^{-1} \cdot \mathbf{h}(\mathbf{x}) \leq p$ for sample-based EW D-optimality.*

S4. Proofs of Main Theorems

Proof of Theorem 2.1. For sample-based EW D-optimality, under Assumptions (A1), (A2), and (B3), due to Lemma S2.3, $\mathcal{F}_{SEW}(\mathcal{X})$ is convex and compact. Due to Assumption (B3), there exists a sample-based EW D-optimal design $\xi_* \in \Xi(\mathcal{X})$. Due to the monotonicity of Ψ (see Assumption (B2)), $\hat{E}\{\mathbf{F}(\xi_*, \boldsymbol{\Theta})\}$ must be a boundary point of $\mathcal{F}_{SEW}(\mathcal{X})$. According to Theorem S2.1, there exists a sample-based EW D-optimal design with no more than $p(p+1)/2$ support points.

Similarly, for integral-based EW D-optimality, under Assumptions (A1), (A3), and (B3), there must exist an EW D-optimal design with no more than $p(p+1)/2$ support points.

According to Section 2.4.2 in Fedorov and Leonov (2014), Assumptions (B1), (B2), and (B4) are always satisfied for D-optimality. The rest parts of Theorem 2.1 are direct conclusions of Theorem 2.2 in Fedorov and Leonov (2014). \square

Proof of Theorem 3.1. Suppose all the predictor functions $\mathbf{h}_1, \dots, \mathbf{h}_{J-1}$ and \mathbf{h}_c defined in (5) are continuous with respect to all continuous factors of $\mathbf{x} \in \mathcal{X}$. Then there exists an $M_x > 0$ due to the compactness of \mathcal{X} , such that, $\|\mathbf{h}_j(\mathbf{x})\| \leq M_x$ and $\|\mathbf{h}_c(\mathbf{x})\| \leq M_x$, for all $j = 1, \dots, J-1$ and $\mathbf{x} \in \mathcal{X}$.

According to Appendix A of Huang et al. (2024), if we further have a bounded $\boldsymbol{\Theta}$, then there exists an $M_{\eta} > 0$, such that, $\|\boldsymbol{\eta}_{\mathbf{x}}\| = \|\mathbf{X}_{\mathbf{x}} \boldsymbol{\theta}\| \leq M_{\eta}$ for all $\boldsymbol{\theta} \in \boldsymbol{\Theta}$ and $\mathbf{x} \in \mathcal{X}$. Then there exist $0 < \delta_x < \Delta_x < 1$, such that, $\delta_x \leq \pi_j^{\mathbf{x}}(\boldsymbol{\theta}) \leq \Delta_x$ for all $j = 1, \dots, J$, $\boldsymbol{\theta} \in \boldsymbol{\Theta}$, and $\mathbf{x} \in \mathcal{X}$. Then there exists an $M_u > 0$, such that, $|u_{st}^{\mathbf{x}}(\boldsymbol{\theta})| \leq M_u$ for all $s, t = 1, \dots, J$, $\boldsymbol{\theta} \in \boldsymbol{\Theta}$, and $\mathbf{x} \in \mathcal{X}$. According to Theorem 2 in Huang et al. (2024), there exists an $M_F > 0$, such that, $\|\mathbf{F}_{st}^{\mathbf{x}}(\boldsymbol{\theta})\| = \|\mathbf{F}_{st}(\mathbf{x}, \boldsymbol{\theta})\| \leq M_F$ for all $s, t = 1, \dots, J$, $\boldsymbol{\theta} \in \boldsymbol{\Theta}$, and $\mathbf{x} \in \mathcal{X}$. As a direct conclusion, the Fisher information of an MLM satisfies Assumption (A3). The rest statements are direct conclusions of Theorem 2.1 and Corollary 3.1. \square

Proof of Theorem 3.2. Suppose all the predictor functions $\mathbf{h} = (h_1, \dots, h_p)^T$ are all continuous with respect to $\mathbf{x} \in \mathcal{X}$, and $\boldsymbol{\Theta}$ is bounded. Then there exist $M_x > 0$ and $M_{\eta} > 0$, such that, $\|\mathbf{h}(\mathbf{x})\mathbf{h}(\mathbf{x})^T\| \leq M_x$ for all $\mathbf{x} \in \mathcal{X}$, and $|\mathbf{h}(\mathbf{x})^T \boldsymbol{\theta}| \leq M_{\eta}$ for all $\mathbf{x} \in \mathcal{X}$ and $\boldsymbol{\theta} \in \boldsymbol{\Theta}$. Since ν is continuous for commonly used GLMs (see, for example, Table 5 in the Supplementary Material of Huang et al. (2025)), there is an $M_F > 0$, such that, $|\mathbf{F}_{st}(\mathbf{x}, \boldsymbol{\theta})| \leq M_F$ for all $s, t = 1, \dots, p$, $\boldsymbol{\theta} \in \boldsymbol{\Theta}$, and $\mathbf{x} \in \mathcal{X}$. As a direct conclusion, the Fisher information of a commonly used GLM satisfies Assumption (A3). The rest statements are direct conclusions of Theorem 2.1 and Corollary 3.1. \square

Proof of Theorem S3.1. According to Theorem 2.1, design ξ is EW D-optimal if and only if $\max_{\mathbf{x} \in \mathcal{X}} d(\mathbf{x}, \xi) \leq p$. By applying Theorem 2 and its proof (see their Lemma 1) of Huang et al. (2024), we obtain

$$\text{tr}(\mathbf{E}_{st} u_{st}^{\mathbf{x}} \mathbf{h}_s^{\mathbf{x}} (\mathbf{h}_t^{\mathbf{x}})^T) = u_{st}^{\mathbf{x}} \text{tr}((\mathbf{h}_t^{\mathbf{x}})^T \mathbf{E}_{st} \mathbf{h}_s^{\mathbf{x}}) = u_{st}^{\mathbf{x}} (\mathbf{h}_t^{\mathbf{x}})^T \mathbf{E}_{st} \mathbf{h}_s^{\mathbf{x}}.$$

Note that $u_{st}^{\mathbf{x}}$ here is either $E\{u_{st}^{\mathbf{x}}(\boldsymbol{\Theta})\}$ or $\hat{E}\{u_{st}^{\mathbf{x}}(\boldsymbol{\Theta})\}$, which is different from Huang et al. (2024). \square

Proof of Theorem S3.2. According to Theorem 2.1, a necessary and sufficient condition for a design ξ to be EW D-optimal is $\max_{\mathbf{x} \in \mathcal{X}} d(\mathbf{x}, \xi) \leq p$, which is equivalent to $\max_{\mathbf{x} \in \mathcal{X}} \text{tr}(\mathbf{F}(\xi)^{-1} \mathbf{F}_{\mathbf{x}}) \leq p$. Then the conclusions are obtained due to (S.5), (S.6), and $\mathbf{F}(\xi) = \mathbf{X}_{\xi}^T \mathbf{W}_{\xi} \mathbf{X}_{\xi}$. \square

S5. Model Selection and Design Comparison for Paper Feeder Experiment

In this section, we provide more details about the model selection process and the designs obtained for the paper feeder experiment, which was carried out at Fuji-Xerox by Y. Norio and O. Akira (Joseph and Wu, 2004). In this experiment, there are eight discrete control factors, namely **feed belt material** (x_1 , Type A or Type B), **speed** (x_2 , 288 mm/s, 240 mm/s, or 192 mm/s), **drop height** (x_3 , 3 mm, 2 mm, or 1 mm), **center roll** (x_4 , Absent or Present), **belt width** (x_5 , 10 mm, 20 mm, or 30 mm), **tray guidance angle** (x_6 , 0, 14, or 28), **tip angle** (x_7 , 0, 3.5, or 7), and **turf** (x_8 , None, 1 sheet, or 2 sheets), one noise factor (**stack quantity**, High or Low) (see also Table 2 in Joseph and Wu (2004)), and one continuous control factor, **stack force**, taking values in $[0, 160]$ according to the original experiment. The noise factor is skipped in this analysis since it is not in control of users and is not significant either (Joseph and Wu, 2004). Following Joseph and Wu (2004), we adopt the 18 level settings of eight discrete control factors obtained by coding level 3 as level 1 in column x_4 of Table 5 in Joseph and Wu (2004).

S5.1 Model selection for paper feeder experiment

For the paper feeder experiment, the summarized response variables include the number of misfeeds y_{i1} , the number of precise feeding of the paper y_{i2} , and the number of multifeeds y_{i3} at the experimental setting \mathbf{x}_i . It is important to notice that these two types of failures, misfeed or multifeed, cannot occur simultaneously. Therefore, a multinomial logistic model is more appropriate than two separate generalized linear models for analyzing this experiment. For those three-level factors, namely x_2, x_3, x_5, x_6, x_7 , and x_8 which are all quantitative factors, we follow Wu and Hamada (2009) and Joseph and Wu (2004) to convert the two degrees of freedom for each factor into linear and quadratic components with contrasts $(-1, 0, 1)$ and $(1, -2, 1)$, respectively. Following Joseph and Wu (2004), we code each of the two-level factors x_1 and x_4 , which are qualitative factors, as $(-1, 1)$. As for the continuous factor stack force M , we transform it to $\log(M + 1)$, which is slightly different from $\log M$ in Joseph and Wu (2004), to deal with a few cases with $M = 0$.

Table S.1: Model comparison for paper feeder experiment

	Cumulative		Continuation		Adjacent		Baseline	
	po	npo	po	npo	po	npo	po	npo
AIC	1011.06	937.87	1037.60	970.59	1027.72	962.99	1661.38	962.99
BIC	1104.34	1113.46	1130.88	1146.18	1121.00	1138.58	1754.66	1138.58

We first use AIC and BIC criteria to choose the most appropriate multinomial logistic model from eight different candidates (Bu et al., 2020). According to Table S.1, we adopt the cumulative logit model with non-proportional odds (npo), which achieves the smallest AIC and BIC values (highlighted in bold font), and is described as follows:

$$\begin{aligned}
\log \frac{\pi_{i1}}{\pi_{i2} + \pi_{i3}} &= \beta_{11} + \beta_{12} \log(M_i + 1) + \beta_{13}x_{i1} + \beta_{14}x_{i2l} + \beta_{15}x_{i2q} + \beta_{16}x_{i3l} + \beta_{17}x_{i3q} \\
&+ \beta_{18}x_{i4} + \beta_{19}x_{i5l} + \beta_{110}x_{i5q} + \beta_{111}x_{i6l} + \beta_{112}x_{i6q} + \beta_{113}x_{i7l} + \beta_{114}x_{i7q} \\
&+ \beta_{115}x_{i8l} + \beta_{116}x_{i8q}, \\
\log \frac{\pi_{i1} + \pi_{i2}}{\pi_{i3}} &= \beta_{21} + \beta_{22} \log(M_i + 1) + \beta_{23}x_{i1} + \beta_{24}x_{i2l} + \beta_{25}x_{i2q} + \beta_{26}x_{i3l} + \beta_{27}x_{i3q} \\
&+ \beta_{28}x_{i4} + \beta_{29}x_{i5l} + \beta_{210}x_{i5q} + \beta_{211}x_{i6l} + \beta_{212}x_{i6q} + \beta_{213}x_{i7l} + \beta_{214}x_{i7q} \\
&+ \beta_{215}x_{i8l} + \beta_{216}x_{i8q},
\end{aligned}$$

where $i = 1, \dots, m$ with $m = 183$ for the original experimental design.

S5.2 Locally D-optimal designs and rounding algorithm for paper feeder experiment

Using the data listed in Table 3 of Joseph and Wu (2004), we fit the chosen model, a cumulative logit model with npo and $p = 32$ parameters. The fitted parameter values are

$$\begin{aligned}\hat{\boldsymbol{\theta}} = & (\hat{\beta}_{11}, \hat{\beta}_{12}, \hat{\beta}_{13}, \hat{\beta}_{14}, \hat{\beta}_{15}, \hat{\beta}_{16}, \hat{\beta}_{17}, \hat{\beta}_{18}, \hat{\beta}_{19}, \hat{\beta}_{110}, \hat{\beta}_{111}, \hat{\beta}_{112}, \hat{\beta}_{113}, \hat{\beta}_{114}, \hat{\beta}_{115}, \hat{\beta}_{116}, \\ & \hat{\beta}_{21}, \hat{\beta}_{22}, \hat{\beta}_{23}, \hat{\beta}_{24}, \hat{\beta}_{25}, \hat{\beta}_{26}, \hat{\beta}_{27}, \hat{\beta}_{28}, \hat{\beta}_{29}, \hat{\beta}_{210}, \hat{\beta}_{211}, \hat{\beta}_{212}, \hat{\beta}_{213}, \hat{\beta}_{214}, \hat{\beta}_{215}, \hat{\beta}_{216})^T \\ = & (7.995, -3.268, -1.275, 1.531, 0.044, -0.156, -0.141, 0.534, -0.261, 0.418, \\ & -1.749, -0.084, -0.207, 0.759, 0.782, 0.356, 10.928, -2.461, -0.409, 0.711, \\ & 0.080, -0.144, -0.120, 0.196, 0.019, -0.023, -0.931, -0.012, -0.133, 0.153, \\ & 0.128, 0.125)^T.\end{aligned}$$

Assuming $\hat{\boldsymbol{\theta}}$ to be the true values of the model parameters, we first apply the ForLion algorithm proposed by Huang et al. (2024) and obtain a locally D-optimal approximate design, which consists of 41 design points and is listed as “ForLion” in both Table S.2 and Table S.4. To convert this approximate design with a continuous factor to an exact design, we apply our rounding algorithm (Algorithm 2) to it with merging threshold $\delta_r = 3.2$, grid level $L = 2.5$, and the number of experimental units $n = 1,785$ (the same sample size as in the original experiment). The obtained exact design is listed as “ForLion exact grid2.5” in Tables S.2 and S.4. For comparison purpose, we also apply the lift-one and exchange algorithms of Bu et al. (2020) to two different sets of design points: one set is the same as the original experiment, and the other is based on the grid points of stack force with pace length 2.5 (that is, $\{0, 2.5, 5, \dots, 157.5, 160\}$) for each of the 18 experimental settings (runs) of the eight discrete factors. The designs obtained correspondingly are presented as “Bu-appro” (lift-one algorithm on original design points) and “Bu-exact” (exchange algorithm on original design points) in Tables S.2 and S.3, and “Bu-grid2.5 appro” (lift-one algorithm on grid-2.5 points) and “Bu-grid2.5 exact” (exchange algorithm on grid-2.5 points) in Tables S.2 and S.4. According to the summarized information of those designs listed in Table S.2, the ForLion design and its exact designs obtained by Algorithm 2 with grid level $L = 0.1, 0.5, 1, 2.5$, respectively, achieve the highest relative efficiencies with respect to the ForLion design itself, as well as the fewest design points. On the contrary, the lift-one and exchange algorithms of Bu et al. (2020) are much more time-consuming even with grid level 2.5, and the original design and Bu’s designs (Bu-appro and Bu-exact) on the original set of design points are not satisfactory in terms of relative efficiency.

Table S.2: Locally D-optimal designs for paper feeder experiment

Designs	m	Time (s)	$ \mathbf{F}(\boldsymbol{\xi}, \boldsymbol{\theta}) $	Relative Efficiency
Original allocation	183	-	1.164e+28	62.792%
Bu-appro	41	62.58s	5.930e+32	88.106%
Bu-exact	41	1598s	5.928e+32	88.105%
Bu-grid2.5 appro	50	81393s	2.397e+34	98.903%
Bu-grid2.5 exact	48	85443s	2.396e+34	98.902%
ForLion	41	22099s	3.411e+34	100.000%
ForLion exact grid-0.1	36	0.01s	3.412e+34	100.001%
ForLion exact grid-0.5	36	0.01s	3.374e+34	99.965%
ForLion exact grid-1	36	0.01s	2.556e+34	99.102%
ForLion exact grid-2.5	36	0.01s	2.245e+34	98.701%

Note: m is the number of design points; Relative Efficiency is $(|\mathbf{F}(\boldsymbol{\xi}, \hat{\boldsymbol{\theta}})|/|\mathbf{F}(\boldsymbol{\xi}_{\text{ForLion}}, \hat{\boldsymbol{\theta}})|)^{1/p}$ with $p = 32$.

The ForLion exact designs (with grid-0.1, grid-0.5, grid-1, and grid-2.5) in Table S.2 also show the convenience by adopting our rounding algorithm (Algorithm 2). Once an optimal approximate design is obtained, the exact design with a user-specified grid level can be obtained instantly with high relative efficiency. To show how we choose the merging threshold $\delta_r = 3.2$ for this experiment, in Figure S.1 we show how the relative efficiency (left panel) and the number of design points (right panel) change along with the relative distance (i.e., the merging threshold δ_r), where the grid levels 0.1, 0.5, 1 and 2.5, and the relative distances between 2 and 6 with increment of 0.1 are used for illustration. Notably, the next change on the number of design points after $\delta_r = 3.2$ will not

occur until $\delta_r = 31.29$, which is too large. As a result, we recommend the merging threshold $\delta_r = 3.2$ for this experiment. The choice of grid level typically depends control accuracy of the factors and the options that the experimenter may have. As illustrated in Table S.2, the experimenter may choose the smallest possible grid level if applicable.

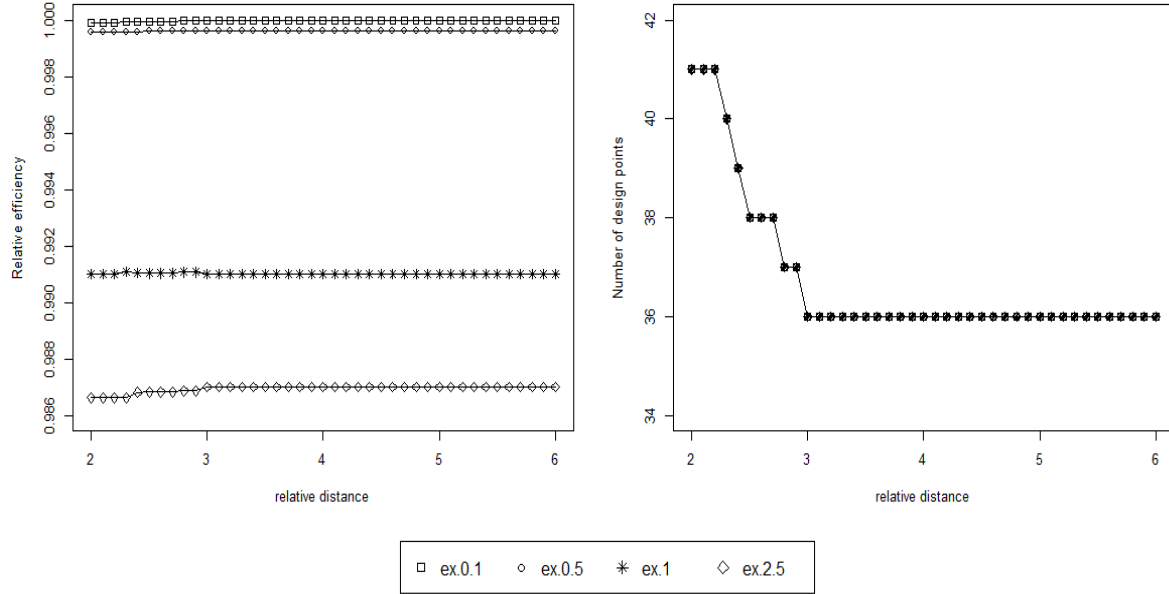


Figure S.1: Relative efficiency and number of design points of exact designs against relative distance (or merging threshold) for paper feeder experiment

S5.3 More graphs and tables for EW D-optimal designs for paper feeder experiment

In this section, we provide (i) Figure S.2 for boxplots of relative efficiencies of different robust designs with respect to locally D-optimal designs, which is a graphical display of Table 2; (ii) Table S.3 for listing designs constructed on the set of design points of the original experiment, including Original (design), Bu-exact by Bu et al. (2020)'s exchange algorithm, Bu-appro by Bu et al. (2020)'s lift-one algorithm, EW Bu-exact by Bu et al. (2020)'s EW exchange algorithm, and EW Bu-appro by Bu et al. (2020)'s EW lift-one algorithm; and (iii) Table S.4 for listing designs constructed on grid points of $[0, 160]$ for stack force.

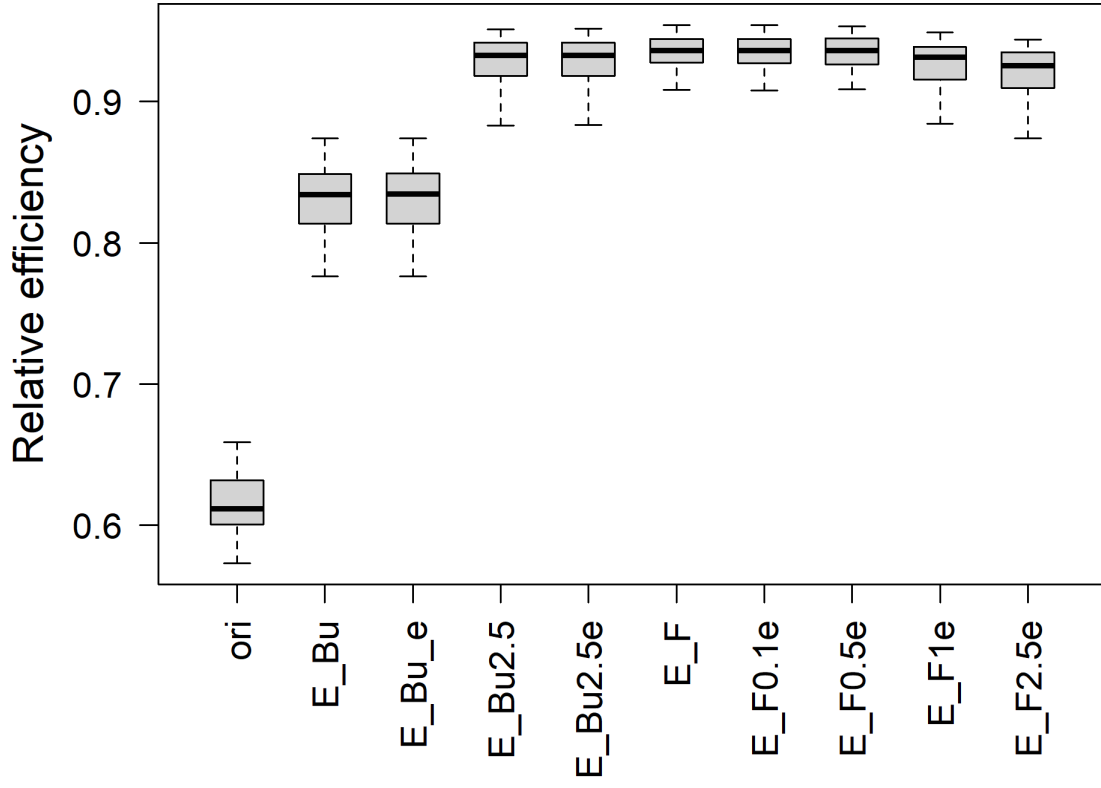


Figure S.2: Boxplots of relative efficiencies of designs in Table 2 with respect to locally D-optimal designs under 100 different sets of parameter values for paper feeder experiment

Table S.3: Designs constructed on the original set of design points for paper feeder experiment

Run	Design	Stack Force																											
		0	5	10	15	20	25	30	35	40	42.5	45	50	55	60	62.5	65	70	75	80	82.5	85	90	95	100	105	110	120	160
1	Original					10		5		10	5	5	10		15	5	5	10		10	5	5	10					5	5
	Bu-exact					59		0		0	0	0	0		0	0	0	0		0	0	0	0				50	0	
	Bu-appro					0.033		0		0	0	0	0		0	0	0	0		0	0	0	0				0.028	0	
	EW Bu-exact					57		0		0	0	0	0		0	0	0	0		0	0	0	0				48	0	
	EW Bu-appro					0.032		0		0	0	0	0		0	0	0	0		0	0	0	0				0.027	0	
2	Original	10		10	10	10		15	5	20			5		15			5	5										
	Bu-exact	0		54	0	0		0	0	0			0		0			0	0	50									
	Bu-appro	0		0.030	0	0		0	0	0			0		0			0	0	0.028									
	EW Bu-exact	0		53	0	0		0	0	0			0		0			0	0	50									
	EW Bu-appro	0		0.029	0	0		0	0	0			0		0			0	0	0.028									
3	Original	15		10	10	20	10	15	5	15																			
	Bu-exact	0		57	0	0	0	0	0	0																			
	Bu-appro	0		0.032	0	0	0	0	0	0	0.025																		
	EW Bu-exact	0		56	0	0	0	0	0	0	43																		
	EW Bu-appro	0		0.031	0	0	0	0	0	0	0.024																		
4	Original	5				10	10	10		15			10	5	15		5	5		5									
	Bu-exact	0				53	0	0		0			0	0	0		0	0		48									
	Bu-appro	0				0.030	0	0		0			0	0	0		0	0		0.027									
	EW Bu-exact	42				49	0	0		0			0	0	0		0	0		47									
	EW Bu-appro	0.024				0.028	0	0		0			0	0	0		0	0		0.026									
5	Original					10	10	15		20			5	20	5	10													
	Bu-exact					58	0	0		0			0	0	0	48													
	Bu-appro					0.033	0	0		0			0	0	0	0.027													
	EW Bu-exact					58	0	0		0			0	0	0	47													
	EW Bu-appro					0.032	0	0		0			0	0	0	0.026													
6	Original				10	10		15		20			5	10	5	5													
	Bu-exact				55	0		0		0			0	0	0	44													
	Bu-appro				0.031	0		0		0			0	0	0	0.025													
	EW Bu-exact				53	0		0		0			0	0	0	43													
	EW Bu-appro				0.030	0		0		0			0	0	0	0.024													
7	Original		10			20	5	20	10	20			5		5			5		5									
	Bu-exact		0			59	0	0	0	0			0		0			0		52									
	Bu-appro		0			0.033	0	0	0	0			0		0			0		0.029									
	EW Bu-exact		0			57	0	0	0	0			0		0			0		50									
	EW Bu-appro		0			0.032	0	0	0	0			0		0			0		0.028									
8	Original			5	10			10	10	10					10			15	5	10					10		5	5	
	Bu-exact				0			14	39	0					0			0	0	0					0		46		
	Bu-appro				0			0.008	0.022	0					0			0	0	0					0		0.026		
	EW Bu-exact				0			0	52	0					0			0	0	0					0		43		
	EW Bu-appro				0			0	0.029	0					0			0	0	0					0		0.024		
9	Original			10	10	10		10		20			5	5	10			5	10		5								
	Bu-exact			0	0	2	53	0		0			0	0	0			0	0	48									
	Bu-appro			0	0	0.001	0.029	0		0			0	0	0			0	0	0.027									
	EW Bu-exact			0	0	0	53	0		0			0	0	0			0	0	46									
	EW Bu-appro			0	0	0	0.030	0		0			0	0	0			0	0	0.026									
10	Original	15	20	15	20	20		10																					
	Bu-exact	0	21	0	0	0		44																					
	Bu-appro	0	0.012	0	0	0		0.025																					
	EW Bu-exact	0	22	0	0	0		44																					
	EW Bu-appro	0	0.013	0	0	0		0.025																					
11	Original	15	20	20	20	20		10																					
	Bu-exact	0	32	0	0	0		44																					
	Bu-appro	0	0.018	0	0	0		0.024																					
	EW Bu-exact	0	30	0	0	0		44																					
	EW Bu-appro	0	0.017	0	0	0		0.024																					
12	Original	10		10	10	10		5		10			5	5						5					5				
	Bu-exact	0		26	33	0		0		0			0	0	0	51				0				0		50			
	Bu-appro	0		0.015	0.018	0		0		0			0	0	0	0.029				0				0		0.028			
	EW Bu-exact	0		27	30	0		0		0			0	0	0	50				0				0		50			
	EW Bu-appro	0		0.015	0.017	0		0		0			0	0	0	0.028				0				0		0.028			
13	Original	10		10	10	10		5		5			5	5						5				5					
	Bu-exact	0		0	58	0		0		0			0	0	0					0				0		50			
	Bu-appro	0		0	0.032	0		0		0			0	0	0					0				0		0.028			
	EW Bu-exact	0		0	56	0		0		0			0	0	0					0				0		50			
	EW Bu-appro	0		0	0.031	0		0		0			0	0	0					0				0		0.028			

Continued on next page

Run	Design	Stack Force																												
		0	5	10	15	20	25	30	35	40	42.5	45	50	55	60	62.5	65	70	75	80	82.5	85	90	95	100	105	110	120	160	
14	Original			10		20	15	20	20	20		5	5																	
	Bu-exact			3		52	0	0	0	0		0	43																	
	Bu-appro			0.002		0.029	0	0	0	0		0	0.024																	
	EW Bu-exact			0		53	0	0	0	0		0	42																	
	EW Bu-appro			0		0.029	0	0	0	0		0	0.024																	
15	Original	10	10	15	15	15		10	5	5		5																		
	Bu-exact	47	0	0	0	0		0	46	0		0																		
	Bu-appro	0.026	0	0	0	0		0	0.026	0		0																		
	EW Bu-exact	46	0	0	0	0		0	46	0		0																		
	EW Bu-appro	0.026	0	0	0	0		0	0.026	0		0																		
16	Original		10	10		15		20	10	15		10	5	10																
	Bu-exact		49	0		0		0	0	0		0	0	45																
	Bu-appro		0.028	0		0		0	0	0		0	0	0.025																
	EW Bu-exact		49	0		0		0	0	0		0	0	45																
	EW Bu-appro		0.027	0		0		0	0	0		0	0	0.025																
17	Original			10		10	5	10		10		5	5							5			5	5	10	5	5			
	Bu-exact			0		51	0	0		0		0	0							0		0	0	0	0	0	0	47		
	Bu-appro			0		0.029	0	0		0		0	0							0		0	0	0	0	0	0	0.027		
	EW Bu-exact			0		51	0	0		0		0	0							0		0	0	0	0	0	0	46		
	EW Bu-appro			0		0.028	0	0		0		0	0							0		0	0	0	0	0	0	0.026		
18	Original			10	5	10		10	5	5				10		5	10	5	10				10							5
	Bu-exact			0	6	53		0	0	0				0		0	0	0	0			51							0	
	Bu-appro			0	0.003	0.030		0	0	0				0		0	0	0	0			0.029							0	
	EW Bu-exact			0	0	57		0	0	0				0		0	0	0	0			50							0	
	EW Bu-appro			0	0	0.032		0	0	0				0		0	0	0	0			0.028							0	

Table S.4: Designs constructed on $[0, 160]$ of stack force for paper feeder experiment

Run	Design	Stack Force				w_i or n_i			
1	Bu-grid2.5	20.0	112.5	-	-	0.0305	0.0264	-	-
	Bu-grid2.5 exact	20.0	112.5	-	-	55	47	-	-
	ForLion	21.839	110.554	-	-	0.0292	0.0270	-	-
	ForLion exact grid2.5	22.5	110.0	-	-	52	48	-	-
	EW Bu-grid2.5	20.0	22.5	110	112.5	0.0173	0.0124	0.0065	0.0189
	EW Bu-grid2.5 exact	20.0	22.5	112.5	-	30	23	45	-
	EW ForLion	22.127	111.339	-	-	0.0288	0.0255	-	-
2	EW ForLion exact grid2.5	22.5	112.5	-	-	51	45	-	-
	Bu-grid2.5	5.0	75.0	-	-	0.0291	0.0279	-	-
	Bu-grid2.5 exact	5.0	75.0	-	-	52	50	-	-
	ForLion	4.749	74.807	-	-	0.0286	0.0280	-	-
	ForLion exact grid2.5	5.0	75.0	-	-	51	50	-	-
	EW Bu-grid2.5	5.0	75.0	77.5	-	0.0284	0.0169	0.0110	-
	EW Bu-grid2.5 exact	5.0	75.0	77.5	-	51	37	13	-
3	EW ForLion	4.505	75.677	-	-	0.0281	0.0280	-	-
	EW ForLion exact grid2.5	5.0	75.0	-	-	50	50	-	-
	Bu-grid2.5	7.5	47.5	-	-	0.0284	0.0257	-	-
	Bu-grid2.5 exact	7.5	47.5	-	-	51	46	-	-
	ForLion	7.669	46.322	-	-	0.0284	0.0261	-	-
	ForLion exact grid2.5	7.5	47.5	-	-	51	47	-	-
	EW Bu-grid2.5	7.5	45.0	47.5	-	0.0279	0.0055	0.0197	-
4	EW Bu-grid2.5 exact	7.5	45.0	47.5	-	50	4	41	-
	EW ForLion	7.735	46.387	-	-	0.0279	0.0252	-	-
	EW ForLion exact grid2.5	7.5	47.5	-	-	50	45	-	-
	Bu-grid2.5	17.5	20.0	97.5	100	0.0055	0.0237	0.0175	0.0084
	Bu-grid2.5 exact	17.5	20.0	97.5	100	10	42	34	12
	ForLion	18.476	97.700	-	-	0.0288	0.0268	-	-
	ForLion exact grid2.5	17.5	97.5	-	-	51	48	-	-
5	EW Bu-grid2.5	0.0	20.0	100.0	102.5	0.0253	0.0270	0.0114	0.0136
	EW Bu-grid2.5 exact	0.0	20.0	100.0	102.5	45	48	5	40
	EW ForLion	0.000	19.984	100.379	-	0.0190	0.0265	0.0242	-
	EW ForLion exact grid2.5	0.0	20.0	100.0	-	34	47	43	-
	Bu-grid2.5	15.0	82.5	-	-	0.0321	0.0287	-	-
	Bu-grid2.5 exact	15.0	82.5	-	-	57	51	-	-
	ForLion	13.925	83.114	-	-	0.0315	0.0294	-	-
6	ForLion exact grid2.5	15.0	82.5	-	-	56	53	-	-
	EW Bu-grid2.5	15.0	82.5	85.0	-	0.0314	0.0245	0.0033	-
	EW Bu-grid2.5 exact	15.0	82.5	-	-	56	50	-	-
	EW ForLion	14.527	83.063	-	-	0.0311	0.0280	-	-
	EW ForLion exact grid2.5	15.0	82.5	-	-	55	50	-	-
	Bu-grid2.5	12.5	15.0	87.5	-	0.0075	0.0229	0.0251	-
	Bu-grid2.5 exact	12.5	15.0	87.5	-	14	40	45	-
7	ForLion	12.212	86.679	-	-	0.0277	0.0259	-	-
	ForLion exact grid2.5	12.5	87.5	-	-	49	46	-	-
	EW Bu-grid2.5	12.5	15.0	85.0	87.5	0.0239	0.0047	0.0046	0.0203
	EW Bu-grid2.5 exact	12.5	15.0	87.5	-	43	8	45	-
	EW ForLion	12.682	87.709	-	-	0.0273	0.0250	-	-
	EW ForLion exact grid2.5	12.5	87.5	-	-	49	45	-	-
	Bu-grid2.5	20.0	92.5	-	-	0.0329	0.0290	-	-
8	Bu-grid2.5 exact	20.0	92.5	-	-	59	52	-	-
	ForLion	18.005	20.767	90.517	-	0.0048	0.0282	0.0299	-
	ForLion exact grid2.5	20.0	90.0	-	-	59	53	-	-
	EW Bu-grid2.5	20.0	90.0	92.5	95.0	0.0322	0.0001	0.0254	0.0023
	EW Bu-grid2.5 exact	20.0	92.5	-	-	57	50	-	-
	EW ForLion	20.206	92.451	-	-	0.0323	0.0277	-	-
	EW ForLion exact grid2.5	20.0	92.5	-	-	58	49	-	-
9	Bu-grid2.5	35.0	160	-	-	0.0275	0.0261	-	-
	Bu-grid2.5 exact	35.0	160	-	-	49	47	-	-
	ForLion	33.541	35.854	160	-	0.0224	0.0048	0.0268	-
	ForLion exact grid2.5	35.0	160	-	-	49	48	-	-
	EW Bu-grid2.5	35.0	160.0	-	-	0.0272	0.0251	-	-
	EW Bu-grid2.5 exact	35.0	160.0	-	-	49	45	-	-
	EW ForLion	33.863	160	-	-	0.0269	0.0252	-	-

Continued on next page

Continued

Run	Design	Stack Force				w_i or n_i			
	EW ForLion exact grid2.5	35.0	160	-	-	48	45	-	-
9	Bu-grid2.5	22.5	25.0	110.0	-	0.0111	0.0199	0.0265	-
	Bu-grid2.5 exact	22.5	25.0	110.0	-	19	36	47	-
	ForLion	24.964	27.906	106.844	-	0.0227	0.0075	0.0275	-
	ForLion exact grid2.5	25.0	107.5	-	-	54	49	-	-
	EW Bu-grid2.5	25.0	112.5	115.0	-	0.0302	0.0160	0.0090	-
	EW Bu-grid2.5 exact	25.0	112.5	-	-	54	45	-	-
	EW ForLion	1.398	26.346	115.877	-	0.0127	0.0275	0.0235	-
	EW ForLion exact grid2.5	2.5	27.5	115.0	-	23	49	42	-
10	Bu-grid2.5	2.5	45.0	-	-	0.0253	0.0247	-	-
	Bu-grid2.5 exact	2.5	45.0	-	-	45	44	-	-
	ForLion	1.573	44.645	-	-	0.0249	0.0247	-	-
	ForLion exact grid2.5	2.5	45.0	-	-	45	44	-	-
	EW Bu-grid2.5	2.5	45.0	-	-	0.0245	0.0247	-	-
	EW Bu-grid2.5 exact	2.5	45.0	-	-	44	44	-	-
	EW ForLion	1.588	44.899	-	-	0.0247	0.0248	-	-
	EW ForLion exact grid2.5	2.5	45.0	-	-	44	44	-	-
11	Bu-grid2.5	2.5	32.5	35.0	-	0.0254	0.0208	0.0038	-
	Bu-grid2.5 exact	2.5	32.5	35.0	-	45	38	6	-
	ForLion	2.105	33.392	-	-	0.0254	0.0247	-	-
	ForLion exact grid2.5	2.5	32.5	-	-	46	44	-	-
	EW Bu-grid2.5	2.5	32.5	-	-	0.0248	0.0245	-	-
	EW Bu-grid2.5 exact	2.5	32.5	-	-	44	44	-	-
	EW ForLion	1.913	33.162	-	-	0.0250	0.0247	-	-
	EW ForLion exact grid2.5	2.5	32.5	-	-	45	44	-	-
12	Bu-grid2.5	12.5	15.0	95.0	97.5	0.0302	0.0004	0.0042	0.0241
	Bu-grid2.5 exact	12.5	15.0	95.0	97.5	54	1	5	46
	ForLion	12.553	96.478	-	-	0.0304	0.0284	-	-
	ForLion exact grid2.5	12.5	97.5	-	-	54	51	-	-
	EW Bu-grid2.5	12.5	92.5	95.0	-	0.0303	0.0120	0.0158	-
	EW Bu-grid2.5 exact	12.5	92.5	95.0	-	54	25	25	-
	EW ForLion	12.194	94.016	-	-	0.0301	0.0279	-	-
	EW ForLion exact grid2.5	12.5	95.0	-	-	54	50	-	-
13	Bu-grid2.5	12.5	15.0	92.5	95.0	0.0187	0.0130	0.0224	0.0061
	Bu-grid2.5 exact	12.5	15.0	92.5	95.0	33	24	41	10
	ForLion	14.693	92.175	-	-	0.0312	0.0287	-	-
	ForLion exact grid2.5	15.0	92.5	-	-	56	51	-	-
	EW Bu-grid2.5	12.5	15.0	92.5	95.0	0.0034	0.0276	0.0098	0.0179
	EW Bu-grid2.5 exact	12.5	15.0	95	-	6	49	49	-
	EW ForLion	14.488	93.508	-	-	0.0306	0.0279	-	-
	EW ForLion exact grid2.5	15.0	92.5	-	-	55	50	-	-
14	Bu-grid2.5	15.0	17.5	77.5	80.0	0.0082	0.0217	0.0025	0.0235
	Bu-grid2.5 exact	15.0	17.5	80	-	14	39	46	-
	ForLion	16.439	18.660	76.924	-	0.0207	0.0090	0.0269	-
	ForLion exact grid2.5	17.5	77.5	-	-	53	48	-	-
	EW Bu-grid2.5	17.5	80.0	82.5	-	0.0291	0.0192	0.0056	-
	EW Bu-grid2.5 exact	17.5	80.0	-	-	52	44	-	-
	EW ForLion	17.449	80.152	-	-	0.0291	0.0249	-	-
	EW ForLion exact grid2.5	17.5	80.0	-	-	52	44	-	-
15	Bu-grid2.5	0.0	32.5	-	-	0.0242	0.0247	-	-
	Bu-grid2.5 exact	0.0	32.5	-	-	43	44	-	-
	ForLion	0.462	32.783	-	-	0.0247	0.0246	-	-
	ForLion exact grid2.5	0.0	32.5	-	-	44	44	-	-
	EW Bu-grid2.5	0.0	32.5	-	-	0.0226	0.0248	-	-
	EW Bu-grid2.5 exact	0.0	32.5	-	-	40	44	-	-
	EW ForLion	0.483	32.917	-	-	0.0245	0.0248	-	-
	EW ForLion exact grid2.5	0.0	32.5	-	-	44	44	-	-
16	Bu-grid2.5	5.0	65.0	-	-	0.0259	0.0246	-	-
	Bu-grid2.5 exact	5.0	65.0	-	-	46	44	-	-
	ForLion	4.119	64.968	-	-	0.0253	0.0247	-	-
	ForLion exact grid2.5	5.0	65.0	-	-	45	44	-	-
	EW Bu-grid2.5	5.0	65.0	-	-	0.0255	0.0248	-	-
	EW Bu-grid2.5 exact	5.0	65.0	-	-	45	44	-	-
	EW ForLion	4.185	64.902	-	-	0.0251	0.0249	-	-

Continued on next page

Continued

Run	Design	Stack Force				w_i or n_i			
	EW ForLion exact grid2.5	5.0	65.0	-	-	45	44	-	-
17	Bu-grid2.5	17.5	142.5	145.0	-	0.0268	0.0015	0.0237	-
	Bu-grid2.5 exact	17.5	145	-	-	48	45	-	-
	ForLion	17.181	144.491	-	-	0.0265	0.0254	-	-
	ForLion exact grid2.5	17.5	145	-	-	47	45	-	-
	EW Bu-grid2.5	17.5	137.5	140.0	142.5	0.0266	0.0005	0.0193	0.0052
	EW Bu-grid2.5 exact	17.5	140	-	-	47	45	-	-
	EW ForLion	17.437	140.331	-	-	0.0262	0.0251	-	-
	EW ForLion exact grid2.5	17.5	140.0	-	-	47	45	-	-
18	Bu-grid2.5	17.5	20.0	92.5	95.0	0.0280	0.0042	0.0115	0.0176
	Bu-grid2.5 exact	17.5	20.0	92.5	95.0	50	7	23	29
	ForLion	17.157	19.653	93.331	-	0.0301	0.0019	0.0298	-
	ForLion exact grid2.5	17.5	92.5	-	-	57	53	-	-
	EW Bu-grid2.5	17.5	92.5	95.0	-	0.0312	0.0123	0.0159	-
	EW Bu-grid2.5 exact	17.5	95	-	-	56	50	-	-
	EW ForLion	17.933	94.525	-	-	0.0314	0.0282	-	-
	EW ForLion exact grid2.5	17.5	95.0	-	-	56	50	-	-

S6. Robustness of Sample-based EW Designs

In this section, we use the minimizing surface defects experiment (see Section 4.2) to illustrate the robustness of sample-based EW D-optimal designs against different sets of parameter vectors.

For illustration purpose, we simulate five random sets of parameter vectors from the prior distributions listed in Table S1 of Huang et al. (2024), denoted by $\Theta^{(k)} = \{\theta_1^{(k)}, \dots, \theta_B^{(k)}\}$, with $B = 1000$, and $k \in \{1, 2, 3, 4, 5\}$. For each $k = 1, \dots, 5$, we obtain the corresponding sample-based EW D-optimal design $\xi^{(k)}$ for the minimizing surface defects experiment, which maximizes $f_{\text{SEW}}(\xi) = |\hat{E}\{\mathbf{F}(\xi, \Theta^{(k)})\}| = |B^{-1} \sum_{j=1}^B \mathbf{F}(\xi, \theta_j^{(k)})|$. The numbers of design points are 15, 13, 21, 19, and 17, respectively.

For $l, k \in \{1, 2, 3, 4, 5\}$, we calculate the relative efficiencies of $\xi^{(l)}$ with respect to $\xi^{(k)}$ under $\Theta^{(k)}$, that is,

$$\left(\frac{|\hat{E}\{\mathbf{F}(\xi^{(l)}, \Theta^{(k)})\}|}{|\hat{E}\{\mathbf{F}(\xi^{(k)}, \Theta^{(k)})\}|} \right)^{1/p}$$

with $p = 10$. The relative efficiencies are shown in the following matrix

$$\begin{matrix} & l=1 & l=2 & l=3 & l=4 & l=5 \\ \begin{matrix} k=1 \\ k=2 \\ k=3 \\ k=4 \\ k=5 \end{matrix} & \begin{pmatrix} 1.00000 & 0.99179 & 0.99586 & 0.99284 & 0.98470 \\ 0.98258 & 1.00000 & 0.98508 & 0.98134 & 0.98117 \\ 0.99078 & 0.98748 & 1.00000 & 0.98165 & 0.98632 \\ 0.97629 & 0.98376 & 0.97910 & 1.00000 & 0.98501 \\ 0.97947 & 0.98850 & 0.98804 & 0.98842 & 1.00000 \end{pmatrix} \end{matrix}$$

with the minimum relative efficiency 0.97629.

By applying the rounding algorithm (Algorithm 2) with merging threshold $L = 1$ and the number of experimental units $n = 1000$, we obtain the corresponding exact designs, whose numbers of design points are still 15, 13, 21, 19, and 17, respectively. Their relative

efficiencies are

	l=1	l=2	l=3	l=4	l=5
k=1	1.00000	0.99144	0.99593	0.99299	0.98448
k=2	0.98287	1.00000	0.98535	0.98174	0.98128
k=3	0.99080	0.98716	1.00000	0.98184	0.98614
k=4	0.97634	0.98359	0.97916	1.00000	0.98488
k=5	0.97959	0.98836	0.98797	0.98846	1.00000

with the minimum relative efficiency 0.97634.

In terms of relative efficiencies, the sample-based EW D-optimal designs for this experiment are fairly robust against the different sets of parameter vectors.

S7. More Examples

In this section, we provide two more examples, including an electrostatic discharge experiment example and a three-continuous-factor artificial example, both under generalized linear models.

S7.1 Electrostatic discharge experiment

An electrostatic discharge (ESD) experiment was considered by Lukemire et al. (2019) and Huang et al. (2024), which involves a binary response, four discrete factors, namely LotA, LotB, ESD, and Pulse, all taking values in $\{-1, 1\}$, and one continuous factor Voltage in $[25, 45]$. The list of factors, corresponding parameters, the nominal values adopted by Lukemire et al. (2019), and the prior distribution adopted by Huang et al. (2024) are summarized in Table S.5. Lukemire et al. (2019) employed a d -QPSO algorithm and derived a locally D-optimal approximate design with 13 support points for a logistic model $Y \sim \text{Bernoulli}(\mu)$ with $\text{logit}(\mu) = \beta_0 + \beta_1 \text{LotA} + \beta_2 \text{LotB} + \beta_3 \text{ESD} + \beta_4 \text{Pulse} + \beta_5 \text{Voltage} + \beta_{34}(\text{ESD} \times \text{Pulse})$. Huang et al. (2024) used their ForLion algorithm and found a slightly better locally D-optimal design in terms of relative efficiency, which consists of 14 design points. Both designs were constructed under the assumption that the nominal values listed in Table S.5 are the true values.

In practice, however, an experimenter may not possess precise parameter values before the experiment. As an illustration, we adopt the prior distributions listed in Table S.5 (i.e., independent uniform distributions) on the model parameters. By applying our EW ForLion algorithm on the same model with the specified prior distribution, we obtain the integral-based EW D-optimal approximate design, and present it on the left side of Table S.6, which consists of 18 design points. Subsequently, we utilize our rounding algorithm with merging threshold $L = 0.1$ and the number of experimental units $n = 100$ (as an illustration) to obtain an exact design, and present it on the right side of Table S.6, which consists of 17 design points (the 18th design point of the approximate design vanishes due to its low weight).

To make comparison, we randomly generate $N = 10,000$ parameter vectors $\{\theta_1, \dots, \theta_N\}$ from the prior distribution listed in Table S.5. For each $j \in \{1, \dots, N\}$ and each

Table S.5: Factors and parameters for electrostatic discharge (ESD) experiment

Type	Factor(Parameter)	Factor Levels/Range	Parameter Prior Distribution	Parameter Nominal Value
	Intercept(β_0)		$U(-8, -7)$	-7.5
Discrete	Lot A (β_1)	$\{-1, 1\}$	$U(1, 2)$	1.5
Discrete	Lot B (β_2)	$\{-1, 1\}$	$U(-0.3, -0.1)$	-0.2
Discrete	ESD (β_3)	$\{-1, 1\}$	$U(-0.3, 0)$	-0.15
Discrete	Pulse (β_4)	$\{-1, 1\}$	$U(0.1, 0.4)$	0.25
Continuous	Voltage (β_5)	[25, 45]	$U(0.25, 0.45)$	0.35
Discrete	ESD \times Pulse (β_{34})	$\{-1, 1\}$	$U(0.35, 0.45)$	0.4

Table S.6: EW D-optimal design (left) and a corresponding exact design (right) for electrostatic discharge (ESD) experiment

Support point	Lot A	Lot B	ESD	Pulse	Voltage	p_i (%)	Support point	$N = 100, L = 0.1$						
								Lot A	Lot B	ESD	Pulse	Voltage	n_i	
1	-1	-1	-1	-1	25	8.48	1	-1	-1	-1	-1	25	8	
2	-1	-1	-1	1	25	8.75	2	-1	-1	-1	1	25	9	
3	-1	-1	1	-1	25	4.1	3	-1	-1	1	-1	25	4	
4	-1	-1	1	1	25	8.56	4	-1	-1	1	1	25	9	
5	-1	1	-1	-1	25	6.9	5	-1	1	-1	-1	25	7	
6	-1	1	-1	1	25	5.15	6	-1	1	-1	1	25	5	
7	-1	1	1	-1	25	9.01	7	-1	1	1	-1	25	9	
8	-1	1	1	1	25	8.45	8	-1	1	1	1	25	8	
9	1	-1	1	-1	25	7.43	9	1	-1	1	-1	25	7	
10	1	1	-1	-1	25	3.56	10	1	1	-1	-1	25	4	
11	1	1	-1	1	25	6.21	11	1	1	-1	1	25	6	
12	1	1	1	-1	25	4.43	12	1	1	1	-1	25	4	
13	1	1	1	1	25	0.9	13	1	1	1	1	25	1	
14	-1	1	1	-1	38.948	7.94	14	-1	1	1	-1	38.9	8	
15	-1	1	-1	-1	34.023	1.57	15	-1	1	-1	-1	34	2	
16	-1	1	-1	1	35.405	3.8	16	-1	1	-1	1	35.4	4	
17	-1	-1	1	-1	37.196	4.55	17	-1	-1	1	-1	37.2	5	
18	-1	1	1	1	33.088	0.22								

ξ under comparison, we compute $(|\mathbf{F}(\xi, \theta_j)|^{1/p} = |\mathbf{X}_\xi^T \mathbf{W}_\xi(\theta_j) \mathbf{X}_\xi|^{1/p}$ with $p = 7$ in this case. In Figure S.3, we present the resulting values as frequency polygons for our EW ForLion design, the locally D-optimal design (“ForLion”) obtained by Huang et al. (2024), and the d -QPSO design (“PSO”) obtained by Lukemire et al. (2019). Compared with ForLion design or PSO design, the frequency polygon for EW ForLion design shows a slightly higher density with low objective functions values, but also a noticeably increased frequency in the higher-value range. Actually, in Table S.7, it clearly shows that the overall mean and median objective function values for EW ForLion designs (approximate and exact designs listed in Table S.6) are higher than ForLion and PSO designs.

Table S.7: Mean and median objective function values based on 10,000 simulated parameter vectors for electrostatic discharge (ESD) experiment

Design	Mean $ \mathbf{X}^T \mathbf{W} \mathbf{X} ^{1/7}$	Median $ \mathbf{X}^T \mathbf{W} \mathbf{X} ^{1/7}$
EW ForLion	0.14677	0.16422
EW ForLion exact	0.14676	0.16410
ForLion	0.14253	0.14990
PSO	0.14187	0.14878

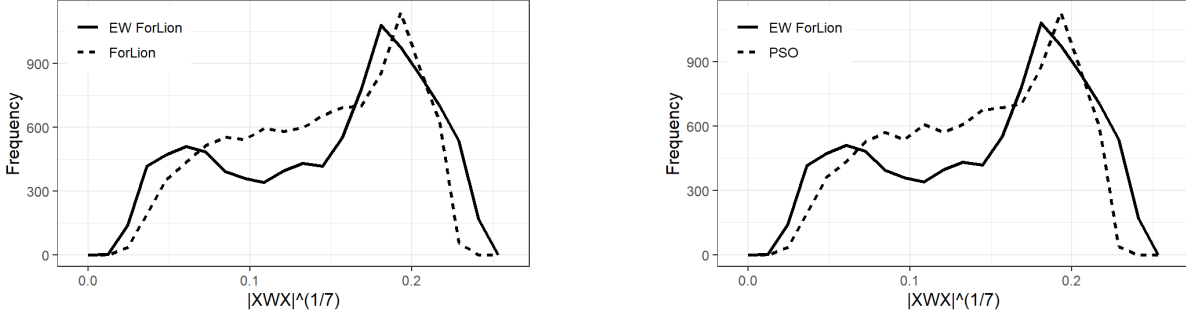


Figure S.3: Frequency polygons of objective function values based on 10,000 simulated parameter vectors for electrostatic discharge experiment

S7.2 A three-continuous-factor example under a GLM

This example refers to Example 4.7 of Stufken and Yang (2012) on a logistic regression model with three continuous factors, represented as $\text{logit}(\mu_i) = \beta_0 + \beta_1 x_{i1} + \beta_2 x_{i2} + \beta_3 x_{i3}$, where the factors were originally defined as $x_{i1} \in [-2, 2]$, $x_{i2} \in [-1, 1]$ and $x_{i3} \in (-\infty, \infty)$.

In this section, for illustration purposes, we reconsider this example by letting $x_{i3} \in [-3, 3]$ and assuming independent priors $\beta_0 \sim N(1, \sigma^2)$, $\beta_1 \sim N(-0.5, \sigma^2)$, $\beta_2 \sim N(0.5, \sigma^2)$, and $\beta_3 \sim N(1, \sigma^2)$, with $\sigma = 1$. Using our EW ForLion algorithm, we obtain an EW D-optimal approximate design, which costs 783 seconds. We further apply our rounding algorithm to the approximate design with $L = 0.0001$ and $n = 100$, and obtain an exact design in just 0.45 second. Remarkably, both designs consist of 7 design points, as detailed in Table S.8, which are different from the 8-point design recommended by Stufken and Yang (2012) with unconstrained x_{i3} .

We compare our designs (“EW ForLion” and “EW ForLion exact-0.0001”) with EW D-optimal designs obtained by applying Bu et al. (2020)’s EW lift-one and exchange algorithms to grid points of continuous factors by discretizing them into 2, 4, 6, 8, and 10 evenly distributed grid points within the corresponding design regions. When the continuous variables are discretized into 10 evenly distributed grid points, Bu et al. (2020)’s EW lift-one and exchange algorithms no longer work due to computational intensity. The summary information of these designs are presented in Table S.9, from which we can see that our EW ForLion algorithm produces a design that is more robust against parameter misspecifications and also requires fewer design points.

Table S.8: EW D-optimal approximate design (left) and exact design (right, $n = 100$) for three-continuous-factor example

Support point	x_1	x_2	x_3	p_i (%)	Support point	x_1	x_2	x_3	n_i
1	-2	-1	-3	7.231	1	-2	-1	-3	7
2	2	-1	-3	20.785	2	2	-1	-3	21
3	-2	1	-1.8	19.491	3	-2	1	-1.8	19
4	2	1	3	2.718	4	2	1	3	3
5	2	1	-0.3321	18.870	5	2	1	-0.3321	19
6	-2	-1	-0.08665	10.951	6	-2	-1	-0.0867	11
7	0.94673	-0.99688	2.99323	19.954	7	0.9467	-0.9969	2.9932	20

Table S.9: Robust designs for three-continuous-factor example

Design	m	Time (s)	$ E\{\mathbf{F}(\boldsymbol{\xi}, \boldsymbol{\Theta})\} $	Relative Efficiency
EW Grid-2	7	0.06s	0.0009563	90.711%
EW Grid-2 exact	7	0.11s	0.0009559	90.700%
EW Grid-4	8	4.33s	0.0012320	96.641%
EW Grid-4 exact	10	5.03s	0.0012314	96.629%
EW Grid-6	8	13.87s	0.0013278	98.469%
EW Grid-6 exact	8	19.20s	0.0013271	98.455%
EW Grid-8	8	37.58s	0.0013562	98.989%
EW Grid-8 exact	9	46.42s	0.0013553	98.973%
EW Grid-10	-	-	-	-
EW Grid-10 exact	-	-	-	-
EW ForLion	7	782.05s	0.0014124	100.000%
EW ForLion exact-0.0001	7	0.45s	0.0014119	99.991%

Note: Relative Efficiency = $(|E\{\mathbf{F}(\boldsymbol{\xi}, \boldsymbol{\Theta})\}|/|E\{\mathbf{F}(\boldsymbol{\xi}_{\text{EWForLion}}, \boldsymbol{\Theta})\}|)^{1/p}$ with $p = 4$; “-” indicates “unavailable” due to computational intensity.